

# A New Basis for Sparse PCA

Fan Chen

Karl Rohe

*Department of Statistics*

*University of Wisconsin-Madison*

*Madison, WI 53706, USA*

FANCHEN@STAT.WISC.EDU

KARLROHE@STAT.WISC.EDU

## Abstract

The statistical and computational performance of sparse principal component analysis (PCA) can be dramatically improved when the principal components are allowed to be sparse in a rotated eigenbasis. For this, we propose a new method for sparse PCA. In the simplest version of the algorithm, the component scores and loadings are initialized with a low-rank singular value decomposition. Then, the singular vectors are rotated with orthogonal rotations to make them approximately sparse. Finally, soft-thresholding is applied to the rotated singular vectors. This approach differs from prior approaches because it uses an orthogonal rotation to approximate a sparse basis. Our sparse PCA framework is versatile; for example, it extends naturally to the two-way analysis of a data matrix for simultaneous dimensionality reduction of rows and columns. We identify the close relationship between sparse PCA and independent component analysis for separating sparse signals. We provide empirical evidence showing that for the same level of sparsity, the proposed sparse PCA method is more stable and can explain more variance compared to alternative methods. Through three applications—sparse coding of images, analysis of transcriptome sequencing data, and large-scale clustering of Twitter accounts, we demonstrate the usefulness of sparse PCA in exploring modern multivariate data.

**Keywords:** dimensionality reduction, orthogonal rotation, sparse principal component analysis, sparse matrix decomposition, independent component analysis

## 1. Introduction

Principal component analysis (PCA), introduced in the early 20th century (Pearson, 1901; Hotelling, 1933), is one of the most prevalent tools in exploratory and unsupervised multivariate data analysis. PCA converts higher-dimensional data into a lower-dimensional space spanned by uncorrelated principal components (PCs), such that most of the variance in the data is kept. It is ubiquitous in PCA, however, that each PC is the linear combination of *all* the input variables, posing challenges to interpretations and applications of PCA, such as in quantitative finance (Jeffers, 1967). To remedy those disadvantages, sparse PCA estimates “sparse” PCs, each consisting of a handful of the original variables, while still enabling dimensionality reductions and explaining variability of the data (Zou and Xue, 2018).

Sparse PCA can be formulated as an optimization problem over the loading coefficients with cardinality constraint, which results in an NP-hard problem in the strong sense (Tillmann and Pfetsch, 2014). In order to circumvent the obstacle (non-convex  $\ell_0$  norm), various methods have been proposed, such as the iconic regression-based approach by Zou et al. (2006), a convex relaxation to semidefinite programming (d’Aspremont et al., 2007), the penalized matrix decomposition framework (Witten et al., 2009), and the generalized power method (Journée et al., 2010). More recently, theoretical developments have covered the consistency (Johnstone and Lu, 2009; Shen

**By allowing for a rotated basis, sparse PCA can explain nearly as much variance as traditional PCA**

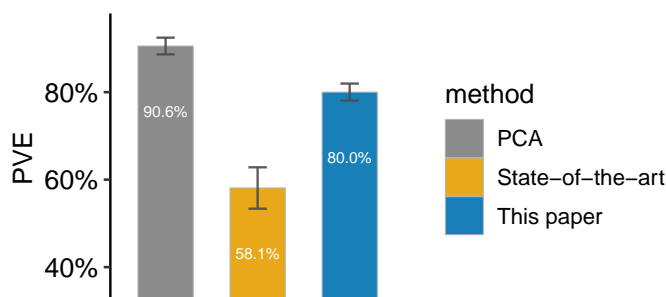


Figure 1: Comparison of explanatory power for the state-of-the-art and the proposed sparse PCA methods. Each bar shows the proportion of variance explained (PVE) by 16 PCs or sparse PCs. The sparse PCs have the same level of sparsity. For both sparse PCA methods, an error bar (based on the three-sigma rule) depicts the variation of PVE over 30 repeated i.i.d. simulations of the data. The state-of-the-art sparse PCA method (yellows) has a limited PVE in the data with larger variation, while the proposed sparse PCA method (blue) possesses a significantly greater PVE with smaller variation. More details about the simulated data and settings are described in Section 5.1.

et al., 2013), variable selection properties (Amini and Wainwright, 2009), rates of convergence, the minimaxity over some Gaussian or sub-Gaussian classes (Vu and Lei, 2013; Cai et al., 2013), and the statistical-computational trade-offs under the restricted covariance concentration condition (Berthet and Rigollet, 2013; Wang et al., 2016) of sparse PCA.

Despite a booming literature of sparse PCA methodologies, there are still several enigmas. First, sparse PCA often explains far less variability in the data than traditional PCA (Figure 1). While this may appear to be a trade-off for sparsity, our results affirm that a substantial improvement is possible. Second, the most common formulations of sparse PCA only estimate a single component at a time and thus rely on a matrix deflation after estimating each component. This deflation entails complications of multiple tuning parameters, non-orthogonality, and sub-optimality (Mackey, 2008). Identifiability and consistency present more subtle issues; there is no reason to assume a priori of distinct eigenvalues or that the gaps between the eigenvalues are small (Vu et al., 2013). Therefore, it seems reasonable to estimate the subspace spanned by multiple sparse PCs, overcoming the dilemma.

Contemporary approaches to sparse PCA primarily focus on presuming the leading eigenvector of the covariance matrix is sparse (e.g., Moghaddam et al. (2006)). To extend the notion of sparse PCA to estimate multiple eigenvectors (or more precisely, the subspace spanned by the leading eigenvectors), Vu and Lei (2013) proposed two notions of subspace sparsity: row sparsity and column sparsity. Row sparsity implies that the eigenvectors themselves are sparse. Column sparsity is an alternative. A column sparse subspace “*is one which has some orthogonal basis consisting of sparse vectors. This means that the choice of basis is crucial; the existence of a sparse basis is an implicit assumption behind the frequent use of rotation techniques by practitioners to help interpret principal components*” (Vu and Lei, 2013). Row sparsity is the most prevalent notion of sparsity used in contemporary sparse PCA, yet it does not appear to describe many contemporary parametric

multivariate models; conversely, many contemporary parametric models in multivariate statistics can be estimated with sparse PCA approaches that can identify column sparsity (Rohe and Zeng, 2020).

In high-dimensional regression, sparse penalties such as the Lasso resolve an invariance; there is an entire space of solutions  $b$  which exactly interpolate the data  $Y = Xb$  and presuming that the solution  $b$  is sparse can make the solution unique. Interestingly, there is no analogue to “sparsity resolving an invariance” for the estimation of row sparse subspace, but there is a very clear analogue in estimating column sparse subspace; the basis is determined by the one that provides the most sparse representation of data.

### 1.1 Our Contributions

In this work, we propose an efficient method, sparse component analysis (SCA), to estimate multiple PCs that are column sparse. Our method allows an orthogonal rotation to the leading singular vectors prior to any sparsity constraints. This is motivated by two facts. First, an orthogonal rotation does not alter the total amount of variance explained by a given set of basis vectors. Second, a good rotation can align the PC loadings with the natural coordinate axes, thus yielding sparse structure (Figure 2). In the psychology literature, it has been a common practice to apply rotations as part of the factor analysis, a close cousin of PCA (Thurstone, 1931; Kaiser, 1960; Jolliffe, 1995). For example, varimax is the most popular option (Kaiser, 1958), which finds the rotation that maximizes the variance of squared loadings. We show in Proposition 1 that when comparing sparse PCA with and without a rotation,

*allowing an orthogonal rotation can only benefit sparse PCA.*

We confirm with numerical evidence that SCA can produce sparse PCs that not only explain a greater amount of variance in the data, but also are stable and robust.

Our framework of SCA generalizes naturally to the two-way analysis of a data matrix for simultaneous dimensionality reduction of rows and columns. For this, we introduce a low-rank matrix approximation method, called sparse matrix approximation (SMA). The SMA is closely related to the penalized matrix decomposition previously proposed in Witten et al. (2009). More importantly, the SMA provides a unified view of sparse PCA and independent component analysis (ICA, see, e.g., Comon, 1994) for sparse sourced signals. ICA is popular and widely studied in the signal processing literature. We show that:

*sparse PCA to a transposed data matrix performs sparse ICA to the original data matrix.*

With such insight, we applied the SCA algorithm to two image processing tasks: the blind source separation and the sparse coding. The results once again confirmed the connection between the two modern multivariate data analysis methods and suggest a broader space of sparse PCA applications.

### 1.2 Organization

The rest of this paper goes as follows. Section 2 describes the SCA method and its variants and extensions. Section 3 provides several algorithmic details. Section 4 illustrates the relationship between SCA and ICA. Section 5 compares different sparse PCA methods through simulation studies. Section 6 demonstrates our methods with several data examples. Section 7 concludes the paper with some discussions.

The same data in seven dimensions, before and after rotation. After the sparse rotation, each PC uses only a small subset of the original variables.

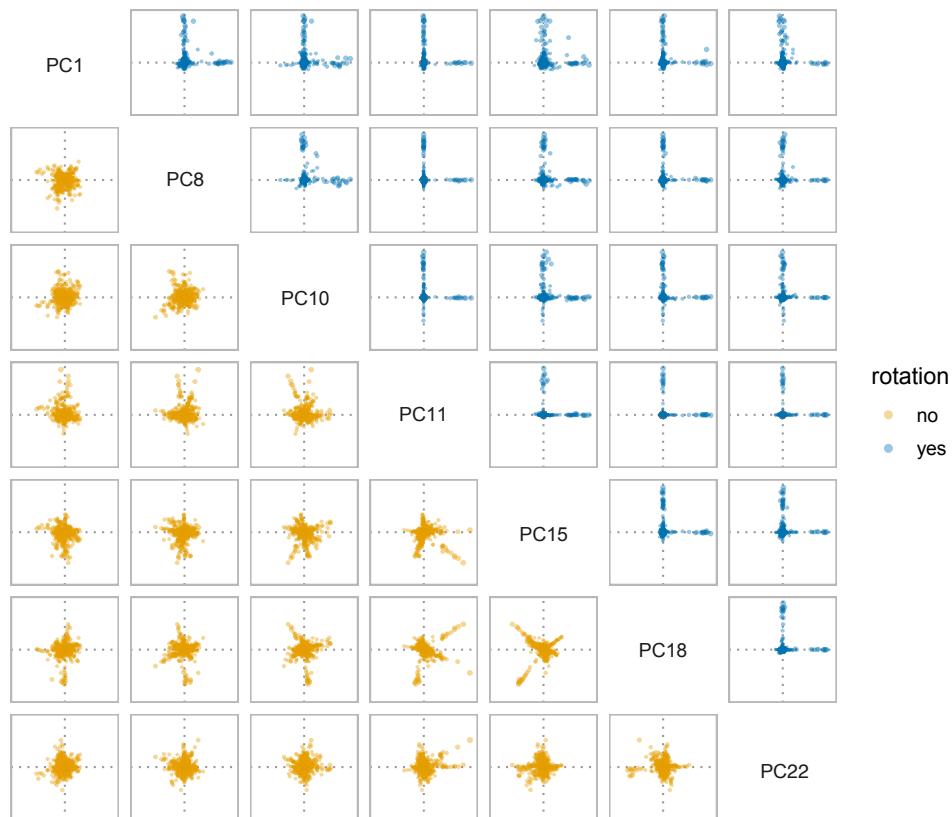


Figure 2: Loadings of seven principal components (PCs). Each (off-diagonal) panel shows the loadings of two PCs on 1,500 original variables (displayed as points). The lower-triangular panels (yellow) depict the PCs without a rotation. The upper-triangular panels (blue) display the PCs with an orthogonal rotation. In each panel, two perpendicular dotted lines (grey) indicate the natural coordinate axes. See Section 6.3 for details about the data analyzed.

### 1.3 Notations

In this paper, the following sets of matrices are frequently considered:  $\mathcal{U}(n) = \{U \in \mathbb{R}^{n \times n} \mid U^T U = I_n\}$  denotes all orthogonal (unitary) matrices in  $\mathbb{R}^n$ , and  $\mathcal{V}(n, k) = \mathcal{V}_k(\mathbb{R}^n) = \{V \in \mathbb{R}^{n \times k} \mid V^T V = I_k\}$  represents the unit Euclidean sphere in  $\mathbb{R}^n$  (also known as the Stiefel manifold), and  $\mathcal{B}(n, k) = \{V \in \mathbb{R}^{n \times k} \mid [V^T V]_{ii} \leq 1, 1 \leq i \leq k\}$  is the unit Euclidean ball (i.e., the convex hull of  $\mathcal{V}(n, k)$ ). Throughout, we discuss the *entrywise* matrix norm only. For any matrix  $A \in \mathbb{R}^{m \times n}$ , its entrywise  $\ell_p$ -norm is defined as  $\|A\|_{p,p} = (\sum_{i=1}^m \sum_{j=1}^n |A_{ij}|^p)^{1/p}$ . In particular, notation  $\|A\|_p$  is also used as the entrywise norm, rather than the norm induced by a vector norm. We note

that the Frobenius norm (or the Hilbert-Schmidt norm) is then an alias of entrywise  $\ell_2$ -norm,  $\|A\|_F = \sqrt{\sum_{i=1}^m \sum_{j=1}^n A_{ij}^2}$ .

## 2. The Methods

Consider a data matrix  $X \in \mathbb{R}^{n \times p}$  of  $n$  observations (or samples) on  $p$  variables. Without loss of generality, we assume that each column of  $X$  is centered (i.e. mean-zero) in this paper. In traditional PCA, the aim is to project  $X$  along  $k$  principal directions (of PCs) that together explain the most variance in the data, that is,

$$\underset{Y}{\text{maximize}} \quad \|XY\|_F \quad \text{subject to} \quad Y \in \mathcal{V}(p, k), \quad (1)$$

where the columns of  $Y$  are called the *loadings*. Because the feasible set is the Stiefel manifold (i.e.,  $\mathcal{V}(p, k)$ ), the columns of  $Y$  are mutually orthogonal and normalized (to unit length). In PCA, each PC is the linear combination of  $p$  original variables, whose coefficients are in the columns of  $Y$ . Note that the coefficients are usually non-zero (i.e.,  $Y$  is usually not sparse). Let  $S = XY \in \mathbb{R}^{n \times k}$  be the transformed data, then  $S_{ij}$  is called the *score* of the  $i$ th sample on the  $j$ th component.

In traditional PCA, the PCs are defined sequentially. That is, for all  $k = 1, 2, \dots, p$ , the loadings of the leading  $k$  PCs are the solution to (1). Such definition, on one hand, ensures the uniqueness of loadings  $Y$ , but on the other hand, coerces the  $k$ th PC to explain the most possible variance in the data, given the preceding  $k - 1$  PCs. While this is required in traditional PCA, we argue that in order for  $k$  sparse PCs whose loadings are presumed *column* sparse, it is sufficient to maximize (1) just for  $k$ . In that case, the solution to (1) becomes a whole space. That is, suppose  $Y^*$  is the optimizer of (1), then  $Y^*R$  is also an optimizer, for any orthogonal matrix  $R \in \mathcal{U}(k)$ . This is truly a desired scenario because it facilitates a searching of the orthogonal rotation that promotes sparse structure (in  $Y^*R$ ). Motivated by such insight, we propose a new method for sparse PCA based on orthogonal rotations and shrinkage.

### 2.1 Sparse Component Analysis

For sparse PCA, we impose an  $\ell_1$  constraint on the PC loadings and define the  $k$  sparse PCs as the solution to the following minimization of matrix reconstruction error:

$$\begin{aligned} & \underset{Z, B, Y}{\text{minimize}} \quad \|X - ZBY^T\|_F \\ & \text{subject to} \quad Z \in \mathcal{V}(n, k), Y \in \mathcal{V}(p, k), \|Y\|_1 \leq \gamma, \end{aligned} \quad (2)$$

where  $\gamma > 0$  is a sparsity controlling parameter (see Section 3.2 for selections of this parameter). In this formulation,  $Y$  corresponds to the loadings, and  $ZB$  corresponds to the scores, and  $Z$  ensures the reconstructed matrix (i.e.,  $ZBY^T$ ) has rank  $k$ . The loadings in  $Y$  are sparse because of the  $\ell_1$ -norm constraint.<sup>1</sup>

The fundamental difference between formulation (2) and previous sparse PCA formulations is the fact that the middle  $B$  matrix is not necessarily diagonal. This added flexibility enables  $Y$  to be column sparse. To see this, suppose the low-rank singular value decomposition (SVD) of  $X$  is  $UDV^T$ , where  $U \in \mathcal{V}(n, k)$ , and  $V \in \mathcal{V}(p, k)$ , and  $D \in \mathbb{R}^{k \times k}$  is a diagonal matrix with the diagonal

1. This constraint can be replaced by other sparsity constraints, e.g., the  $\ell_0$ -norm analogue.

entries in decreasing order, and  $k$  is the approximation rank. Let  $Z = UO$ ,  $B = O^TDR$ , and  $Y = VR$ , for any orthogonal matrices  $O, R \in \mathcal{U}(k)$ . Then,  $ZBY^T$  performs as good as the low-rank SVD in terms of the matrix reconstruction error,

$$\|X - ZBY^T\|_F = \|X - UDV^T\|_F.$$

Here,  $Y$  can be think of as the orthogonally rotated singular vectors. It follows that by allowing the loadings to be sparse in a rotated basis (i.e.,  $\|Y\|_1 \leq \gamma$ ), our formulation in (2) considers column sparse PCA. Furthermore, it can be seen that column sparse PCA is more general. In fact, if  $B$  is restricted to diagonal, (i.e. both  $O$  and  $R$  equal the identity matrix), the formulation (2) reduces to row sparse PCA. The next proposition compares column and row sparse PCA in terms of the matrix reconstruction error.

**Proposition 1 (Effects of orthogonal rotations)** *Let  $X \in \mathbb{R}^{n \times p}$  be any matrix. Suppose  $S_Z$  and  $S_Y$  are two feasible sets for  $Z \in \mathbb{R}^{n \times k}$  and  $Y \in \mathbb{R}^{p \times k}$  respectively, where  $k \leq \min(n, p)$ . Then,*

$$\min_{Z, B, Y} \|X - ZBY^T\|_F \leq \min_{Z, D, Y} \|X - ZDY^T\|_F$$

*subject to  $Z \in S_Z$ ,  $Y \in S_Y$ , and  $D$  is diagonal.*

A proof of Proposition 1 is provided in Appendix A. Proposition 1 says that the additional orthogonal rotations, which are absorbed by the middle  $B$  matrix, allow (column) sparse PCA to explain more variance in the data.

### 2.1.1 COMPUTING SCA

The following lemma translates (2) into an equivalent and more convenient form.

**Lemma 2 (Bilinear form of SCA)** *Solving the minimization in (2) is equivalent to solving the following maximization problem,*

$$\underset{Z, Y}{\text{maximize}} \quad \|Z^TXY\|_F \quad \text{subject to } Z \in \mathcal{V}(n, k), Y \in \mathcal{V}(p, k), \|Y\|_1 \leq \gamma. \quad (3)$$

*In particular, for the optimizer in (2),  $B = Z^TXY$ .*

A proof can be found in Appendix A. Lemma 2 offers three insights to our sparse PCA formulation, which we remark in order:

**Uniqueness.** The objective function in (3) is invariant in any orthogonal rotation to  $Y$  from the right.

Given  $Y \in \mathcal{V}(p, k)$ , the objective value in (3) is the same at  $Y$  and  $YR$  for any orthogonal matrix  $R \in \mathcal{U}(k)$ . However, using the Lagrange form of the constraints on  $Y$  (rather than the bound form),

$$\underset{Z, Y}{\text{minimize}} \quad -\|Z^TXY\|_F + \lambda\|Y\|_1 \quad \text{subject to } Z \in \mathcal{V}(n, k), \quad (4)$$

it can be seen that the optimizer also minimizes  $\|Y\|_1$ . As such, a sufficiently small sparsity parameter  $\gamma$  encourages the solution  $\tilde{Y}$  to be rotated so that  $\|\tilde{Y}\|_1$  is small (and likely sparse). Since  $\|YR\|_1$  is also invariant in column permutation of  $R$ , our sparse PCA formulation does not uniquely order PCs. To resolve this, we describe an ordering of sparse PCs based on the data variance explained by each PC in Section 3.1.

**Existence.** Due to the non-convexity of  $\ell_2$ -equality constraint ( $Z \in \mathcal{V}(n, k)$  and  $Y \in \mathcal{V}(p, k)$ ), the problem is not convex in general, but if we replace the feasible set with its convex hull using  $\ell_2$ -inequality constraints, the optimization problem (3) becomes

$$\underset{Z, Y}{\text{maximize}} \quad \|Z^T XY\|_F \quad \text{subject to} \quad Z \in \mathcal{B}(n, k), Y \in \mathcal{B}(p, k), \|Y\|_1 \leq \gamma. \quad (5)$$

Moreover, due to the Karush-Kuhn-Tucker conditions (see, e.g., Nocedal and Wright, 2006), one could expect the solution to fall on the boundary (i.e., the Stiefel manifold) so long as the sparsity parameters are properly chosen, such that the solution has  $\ell_2$ -norm greater or equal to 1. We describe the reasonable range for sparsity parameters in Section 3.2.

**Bilinearity.** The objective function in (5) is biconvex in  $Z$  and  $Y$ . In fact, with  $Y$  fixed, this criterion takes the form

$$\underset{Z}{\text{maximize}} \quad \|Z^T XY\|_F \quad \text{subject to} \quad Z \in \mathcal{B}(n, k). \quad (6)$$

With  $Z$  fixed, the criterion takes the form

$$\underset{Y}{\text{maximize}} \quad \|Z^T XY\|_F \quad \text{subject to} \quad Y \in \mathcal{B}(p, k), \|Y\|_1 \leq \gamma. \quad (7)$$

The bilinearity suggests an iterative procedure for updating  $Z$  by solving (6) and updating  $Y$  by solving (7) in turns.

### 2.1.2 AN ALGORITHM FOR SCA

Next, we describe an algorithm that computes sparse PCs as formulated in (5). The algorithm of SCA takes a data matrix  $X$ , the sparsity parameters  $\gamma$ , and the desired number of sparse PCs  $k$  as input and outputs the loadings of sparse PCs. The SCA algorithm initializes  $Z \in \mathcal{V}(n, k)$  and  $Y \in \mathcal{V}(p, k)$  with the top  $k$  left and right singular vectors of  $X$  respectively. Once initialized, the algorithm iteratively updates  $Z$  and  $Y$  until convergence.

The update for  $Z$  with fixed  $Y$  is algebraic. The following lemma hints a class of solutions to (6), which is extended from Theorem 7.3.2 in Horn and Johnson (1985).

**Lemma 3 (Maximization without sparsity constraint)** *Given a full-rank matrix  $X \in \mathbb{R}^{n \times p}$ , with  $p \leq n$ , let the singular values of  $X$  be  $\sigma_i$  for  $i = 1, 2, \dots, p$ . Then,*

$$\max_{Y \in \mathcal{V}(n, p)} \|X^T Y\|_F = \sum_{i=1}^p \sigma_i$$

*with the maximizer  $Y^* = \text{polar}(X)$ , up to any orthogonal rotation from the right. Here,  $\text{polar}(X) = X(X^T X)^{-1/2}$ .*

A straightforward proof of Lemma 3 is included in Appendix A for completeness. In Lemma 3, the polar of a matrix  $C \in \mathbb{R}^{n \times p}$ ,  $\text{polar}(C)$ , can be calculated in  $\mathcal{O}(np)$  time (Journée et al., 2010). According to Lemma 3, the SCA algorithm updates  $Z$  with the polar of  $XY$ ,

$$\hat{Z} = \text{polar}(XY).$$

<p><b>Input:</b> <math>A \in \mathbb{R}^{p \times k}</math>          sparsity parameter <math>\gamma</math> (optional, default to <math>\sqrt{pk}</math>)</p>	// Section 3.2
<b>Procedure</b> PRS( $A$ ):	
$\tilde{Y} \leftarrow$ left singular vectors of $A$	
$Y^* \leftarrow$ rotate $\tilde{Y}$ with varimax	// Section 3.3
$\hat{Y} \leftarrow$ soft-threshold $Y^*$ with parameter $\gamma$	// Section 3.4
<b>Output:</b> $\hat{Y}$	

**Algorithm 1:** Polar-Rotate-Shrink (PRS)

<b>Input:</b> data matrix $X$ and a number of components $k$	
<b>Procedure</b> SCA( $X, k$ ):	
initialize $\hat{Z}$ and $\hat{Y}$ with the top $k$ left and right singular vectors of $X$	
<b>repeat</b>	
$\hat{Y} \leftarrow$ PRS( $X^T \hat{Z}$ )	// Algorithm 1
$\hat{Z} \leftarrow$ polar( $X \hat{Y}$ )	// Lemma 3
<b>until</b> convergence	
<b>Output:</b> sparse loadings $\hat{Y}$	

**Algorithm 2:** Sparse Component Analysis (SCA)

To update  $Y$  fixing  $Z$ , we first solve the non-sparse version of (7) (i.e., remove the sparsity constraint  $\|Y\|_1 \leq \gamma$ ),

$$\underset{Y}{\text{maximize}} \quad \|Z^T X Y\|_F \quad \text{subject to } Y \in \mathcal{B}(p, k). \quad (8)$$

Note that the solutions to (8), e.g.,  $\tilde{Y} = \text{polar}(X^T Z)$ , form a subspace in  $\mathcal{V}(p, k)$ , that is, for any orthogonal matrix  $R \in \mathcal{U}(k)$ ,  $\tilde{Y}R$  is also a solution. To further consider the sparsity constraint on  $Y$ , we specifically look for a rotated solution to (8) with the minimal  $\|\tilde{Y}R\|_1$ . However,  $\|Y\|_1$  is not a smooth function of  $Y$  if it contains at least one zero entry. For stable computation, the SCA algorithm instead minimizes a smoother criterion based on the  $\ell_{4/3}$  norm:

$$\underset{R}{\text{minimize}} \quad \|\tilde{Y}R\|_{\frac{4}{3}} \quad \text{subject to } R \in \mathcal{U}(k). \quad (9)$$

This objective coincides the varimax criterion that is ubiquitously applied in factor analysis (Kaiser, 1958). We provide a mathematical derivation for why the varimax rotation may minimize (9) and introduce another rotation method for directly minimizing  $\|\tilde{Y}R\|_1$  in Section 3.3. Let  $Y^* = \tilde{Y}R^*$  be one of the solutions to (8), where  $R^*$  is the solution to (9) in particular. Finally, the algorithm of SCA projects  $Y^*$  onto the feasible set in (7) by soft-thresholding the elements of  $Y^*$  (Donoho, 1995). We explain this choice mathematically under an orthogonal design case and provide some general properties of it in Section 3.4. In summary, we update  $Y$  in three steps—“Polar-Rotate-Shrink” (PRS)—first, find a solution to the maximization problem (8); then, rotate with varimax; finally, soft-threshold all of the elements (Algorithm 1). The PRS module is repeatedly invoked by the SCA algorithm (Algorithm 2) for updating  $Y$ .



### 2.1.3 CONNECTIONS TO OTHER SPARSE PCA METHODS

A distinctive component in the algorithm of SCA is the orthogonal rotation. More broadly, the formulation of SCA in (3) is closely related to many previous sparse PCA formulations, but the possibility of orthogonal rotations has attracted little attention. In this section, we relate and contrast several popular methods to ours, among the plethora of available sparse PCA proposals.

**SPCA (Zou et al., 2006)** SPCA is motivated to maximize the explained variance in the data (Jolliffe et al., 2003). The formulation of SPCA minimizes a “residual sum of squares plus penalties” type of criterion,

$$\underset{U, V}{\text{minimize}} \quad \|X - XVU^T\|_F^2 + \lambda_1 \|V\|_F^2 + \lambda_2 \|V\|_1 \quad \text{subject to } U \in \mathcal{V}(p, k),$$

where  $V \in \mathbb{R}^{p \times k}$  is the sparse loadings of interest, and  $\lambda_1$  and  $\lambda_2$  are tuning parameters. We note that the first part in the objective function is also invariant to any orthogonal rotation applied to  $U$  and  $V$ , because for any  $R \in \mathcal{U}(k)$ , it holds that  $\|X - XVU^T\|_F^2 = \|X - X(VR)(UR)^T\|_F^2$ . Since the algorithm of SPCA is adapted from elastic net (Zou and Hastie, 2005), however, the updates for  $U$  and  $V$  do not use orthogonal rotations to search over the space of feasible solutions.

**SPC (Witten et al., 2009)** SPC finds one sparse PC at a time,

$$\underset{u, v}{\text{maximize}} \quad u^T X v \quad \text{subject to } \|v\|_1 \leq \gamma, \|u\|_2 = 1, \|v\|_2 = 1,$$

where  $u \in \mathbb{R}^n$ , and  $v \in \mathbb{R}^p$  is the single sparse PC of interest. When  $k = 1$ , our formulation of SCA in (3) takes the same form as the SPC formulation, where an orthogonal rotation is unnecessary. However, when  $k > 1$ , SPC does not use an orthogonal rotations, as it aims for sparse PCs sequentially and separately, unlike SCA that computes the sparse PCs all together. SPC is similar to rSVD proposed by Shen and Huang (2008) and TPower proposed by Yuan and Zhang (2013). All the three methods rely on a deflation technique for multiple PCs, which entails complications of, for example, non-orthogonality and sub-optimality (Mackey, 2008). These methods can each be viewed as a special case of the following GPower formulation.

**GPower (Journée et al., 2010)** The block version of GPower aims for multiple sparse PCs simultaneously by considering a linear combination of individual sparse PCA (as formulated in SPC),

$$\underset{U, V}{\text{maximize}} \quad \sum_{i=1}^k \mu_i u_i^T X v_i - \sum_j \lambda_j \|v_j\|_1 \quad \text{subject to } U \in \mathcal{B}(n, k), V \in \mathcal{V}(p, k),$$

where  $V$  is the loadings of sparse PCs of interest, and  $u_j$  and  $v_j$  are the  $j$ th column of  $U$  and  $V$  respectively, and  $\mu_j$  is the weight for the  $j$ th sparse PC, and  $\lambda_j$  is the sparsity tuning parameter for the  $j$ th sparse PC. The algorithm of GPower fundamentally deals with sparse PCs individually, which prohibits orthogonal rotations (on  $V$ ).

**SPCArt (Hu et al., 2016)** SPCArt is the first (to the best of our knowledge) sparse PCA method that concerns orthogonal rotations in its formulation. It searches for sparse PCs by directly

approximating the singular vectors (as opposed to minimizing the reconstruction error or maximizing the explained variance),

$$\underset{Y,R}{\text{minimize}} \quad \|V - YR\|_F^2 + \lambda \|Y\|_1 \quad \text{subject to } Y \in \mathcal{V}(p, k), R \in \mathcal{U}(k),$$

where  $Y$  is the sparse loadings of interest, and  $V \in \mathcal{V}(p, k)$  contains the top  $k$  singular vectors of  $X$ . Conceptually, introducing an orthogonal rotation ( $R$ ) allows a larger searching space for  $Y$ . However, the algorithm of SPCArt does not specifically update  $R$  to promote sparsity (e.g., minimize  $\|Y\|_1$  as in SCA); instead, SPCArt simply computes  $R$  so as to align the polar of  $V$  and  $Y$  (i.e.,  $\hat{R} = \text{polar}(Y^T V)$ ). While this approach is innovative and easy to compute, SPCArt yields performance that is nearly comparable to the GPower based method, as concluded by the authors.

## 2.2 Sparse Matrix Approximation

In this section, we extend SCA to a two-way matrix approximation for simultaneous dimensionality reduction of rows and columns. For this, we propose the sparse matrix approximation (SMA) of a data matrix into  $ZBY^T$ , where  $Z \in \mathbb{R}^{n \times k}$  and  $Y \in \mathbb{R}^{p \times k}$  are sparse, and the middle  $B \in \mathbb{R}^{k \times k}$  matrix contains the basis rotations that enable both  $Z$  and  $Y$  to be sparse. Because  $B$  contains these rotations, it is neither diagonal nor sparse. We formulate SMA as the following reconstruction error minimization problem:

$$\begin{aligned} \underset{Z,B,Y}{\text{minimize}} \quad & \|X - ZBY^T\|_F & (10) \\ \text{subject to} \quad & Z \in \mathcal{B}(n, k), \mathcal{P}_1(Z) \leq \gamma_z, \\ & Y \in \mathcal{B}(p, k), \mathcal{P}_2(Y) \leq \gamma_y, \end{aligned}$$

where  $\gamma_z > 0$  and  $\gamma_y > 0$  are sparsity controlling parameters, and  $\mathcal{P}_1$  and  $\mathcal{P}_2$  are some convex *penalty* functions. If  $\gamma_z$  is sufficiently large, then this is equivalent to (5). Similar to Lemma 2, we transform (10) to an equivalent maximization problem (the proof is almost identical to that of Lemma 2 thus is omitted),

$$\begin{aligned} \underset{Z,Y}{\text{maximize}} \quad & \|Z^T XY\|_F & (11) \\ \text{subject to} \quad & Z \in \mathcal{B}(n, k), \mathcal{P}_1(Z) \leq \gamma_z, \\ & Y \in \mathcal{B}(p, k), \mathcal{P}_2(Y) \leq \gamma_y. \end{aligned}$$

The two criteria in (10) and (11) are equivalent if and only if  $B = Z^T XY$ . This condition suggests that  $B$  can be viewed as the “scores” of SMA, because the sum of squares of its elements determines the matrix reconstruction error, that is,  $\|X\|_F - \|B\|_F$  (see the proof of Lemma 2).

The formulation of SMA in (10) is rooted from the matrix approximation literature. For example, we show that SMA generalizes the penalized matrix decomposition (PMD) proposed by Witten et al. (2009), which is also similar to the method of Shen and Huang (2008). The PMD also decomposes a low-rank data matrix  $X \in \mathbb{R}^{n \times p}$  into three parts,  $ZDY^T$ , where  $Z \in \mathcal{V}(n, k)$  and  $Y \in \mathcal{V}(p, k)$  are presumed sparse, and  $D \in \mathbb{R}^{k \times k}$  is a diagonal matrix whose diagonal entries are in decreasing order, and  $k$  is the rank of the matrix approximation. In order for sparsity, some penalty functions are

**Input:** data matrix  $X \in \mathbb{R}^{n \times p}$  and the approximation rank  $k$

**Procedure SMA** ( $X, k$ ):

initialize  $\hat{Z}$  and  $\hat{Y}$  with the top  $k$  left and right singular vectors of  $X$

**repeat**

$\hat{Z} \leftarrow \text{PRS}(X\hat{Y})$  // Algorithm 1

$\hat{Y} \leftarrow \text{PRS}(X^T\hat{Z})$  // Algorithm 1

**until** *convergence*

$\hat{B} \leftarrow \hat{Z}^T X \hat{Y}$

**Output:**  $\hat{Z}$ ,  $\hat{B}$ , and  $\hat{Y}$

**Algorithm 3:** Sparse Matrix Approximation (SMA) with  $\mathcal{P}_1(A) = \mathcal{P}_2(A) = \|A\|_1$ .

applied to  $Z$  and  $Y$ , which results in the matrix reconstruction error minimization formulation:<sup>2</sup>

$$\begin{aligned} & \underset{U, D, V}{\text{minimize}} && \|X - ZDY^T\|_F \\ & \text{subject to} && Z \in \mathcal{B}(n, k), \mathcal{P}_1(Z) \leq \gamma_z, \\ & && Y \in \mathcal{B}(p, k), \mathcal{P}_2(Y) \leq \gamma_y, \\ & && D \text{ is diagonal,} \end{aligned}$$

where  $\gamma_z, \gamma_y > 0$  are parameters that control the sparsity of  $Z$  and  $Y$ , and  $\mathcal{P}_1$  and  $\mathcal{P}_2$  are some convex penalty function (e.g.  $\ell_1$ -norm). It can be readily seen that SMA generalizes PMD by removing the diagonal constraint on the middle  $D$  matrix. In fact, Proposition 1 suggests that the reconstruction error of SMA is less or equal to that of PMD (see Remark 4 in Appendix A). Another difference between SMA and PMD is in their algorithms. Witten et al. (2009) proposed to find the solution by sequentially maximizing  $[Z^T XY]_{ii}$  for  $i = 1, 2, \dots, k$ , while solving the SMA in (11) amounts to maximizing  $\|Z^T XY\|_F$ . Hence, SMA considers not only the diagonal but also the off-diagonal elements of the scores (i.e.,  $Z^T XY$ ).

Next, we derive an algorithm for SMA. The bilinear objective function in (11) suggests an alternating and iterative algorithm for solving it. Specifically, to update either of  $Z$  and  $Y$  fixing one another, the sparsity-enabling PRS module can be applied. For example, Algorithm 3 outlines an algorithm for computing the SMA with the  $\ell_1$ -norm penalty,  $\mathcal{P}_1(A) = \mathcal{P}_2(A) = \|A\|_1$ . This algorithm is by large the same as Algorithm 2, except that it additionally borrows the PRS module (Algorithm 1) for the update of  $Z$  and that in the end of the algorithm, the scores of SMA is estimated as  $\hat{B} = \hat{Z}^T X \hat{Y}$ . As a result, Algorithm 3 outputs the estimates  $\hat{Z}$ ,  $\hat{B}$ , and  $\hat{Y}$ .

### 2.3 Other Variants and Extensions

The general framework of SCA, especially the orthogonal rotation component, is versatile. In this section, we list a few variants and extensions of this framework.

**Vintage Sparse PCA** Although the algorithm of SCA is iterative, we found that one iteration often yields a good approximation. We refer to the SCA algorithm with one iteration as *vintage sparse PCA* (VSP) as studied in Rohe and Zeng (2020). Note that in VSP, the soft-thresholding

---

2. The paper originally considers the PMD with  $k = 1$ . The PMD finds multiple factors sequentially using a deflation technique.

is less essential. In Section 6.3, we apply VSP to a targeted sample of the Twitter friendship network to identify communities of Twitter accounts (Chen et al., 2020; Zhang et al., 2020).

**Sparse Coding** Another variant of PCA concerns sparse coding for individual samples, where instead of loadings of PCs, we presume sparse component scores. In PCA with  $k$  PCs, the component scores represent each data point in  $\mathbb{R}^k$ . So, component scores being sparse suggests that each point is correlated with only a small subset of PCs. This variant is particularly meaningful when the number  $k$  of PCs is large and the individual samples are presumed to have some sparse structure. To formulate sparse coding, it can be viewed as a special case of the SMA in (10), where the sparsity constraint on  $Y$  is omitted.<sup>3</sup> It can thus be seen that sparse coding can be solved using the SCA algorithm. For sparse coding, we perform SCA on the transposed data matrix, then the resulting sparse loadings estimate is in fact an estimate of sparse component scores for the original data. In fact, sparse coding is very similar to independent component analysis. We elaborate this connection in Section 4 and provide examples in Section 6.1.

**Sparse CCA** Canonical correlation analysis (CCA) correlates two sets of multivariate data by applying linear transformations to each (Hotelling, 1936). In the analysis of high-dimensional data (e.g., genomic data), the linear transformations are preferred to be sparse. The mathematical formulation of CCA requires simultaneous row and column dimensionality reductions, for which the SMA framework is immediately applicable to it (see Appendix B for a mathematical formulation).

### 3. Algorithmic Details

In this section, we provide some details about the algorithms of SCA and SMA.

#### 3.1 Ordering Sparse PCs

In PCA, the PCs are ordered. However, the formulation of SCA does not imply an order for sparse PCs. To bridge this gap, we order the sparse PCs by their explained variance (EV) in the data. For PC  $y_i \in \mathbb{R}^p$ , the EV is defined as  $\|Xy_i\|_2^2$ . Note that the output of sparse PC loadings may not be strictly orthogonal. So, after this ordering, we then calculate the cumulative proportion of variance explained (PVE) by the leading  $k$ th sparse PCs. The PVE is previously introduced by Shen and Huang (2008) and is defined as  $\|X_Y\|_F^2$ , where  $X_Y = XY(Y^T Y)^{-1} Y^T$ .

#### 3.2 Choosing the Sparsity Parameter

Both SCA and SMA contain sparsity parameters ( $\gamma$ ). First, for  $Y \in \mathcal{V}(p, k)$  and the sparsity constraint  $\|Y\|_1 \leq \gamma$ , we restrict our discussion to  $k \leq \gamma \leq k\sqrt{p}$ . This is because if  $\gamma > k\sqrt{p}$ , the sparsity constraint becomes inactive, then the solution will not necessarily be sparse (Figure 3 left panel). Similar, condition  $\gamma > k$  renders the solution on (or near) the Stiefel manifold  $\mathcal{V}(p, k)$ ,

---

3. The SMA is not a variant of PCA with simultaneously sparse component scores and loadings. In fact, the middle  $B$  matrix in the SMA is absorbed by either component scores (in SCA) or loadings (in sparse coding) and results in non-sparsity respectively.

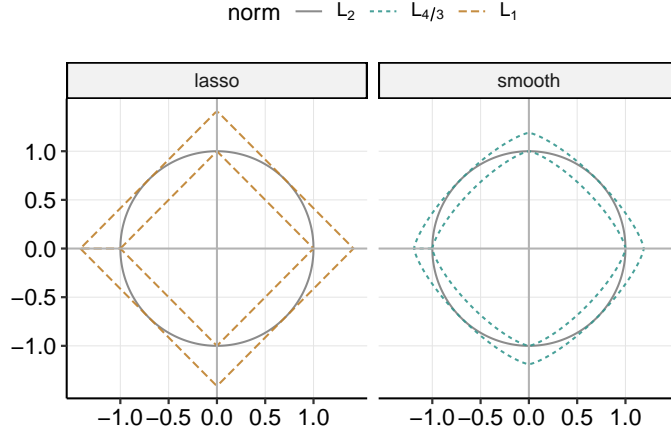


Figure 3: Comparison of the  $\ell_p$  norms. Left: Two  $\ell_1$ -norm contours of 1 and  $\sqrt{2}$  in brown dashed line and the  $\ell_2$ -norm contour of 1 in grey solid line. Right:  $\ell_{4/3}$ -norm contours of 1 and  $2^{1/4}$  in green dotted line and the  $\ell_2$ -norm contour of 1 in grey solid line.

hence, it can help the solution to be orthogonal.<sup>4</sup> Similarly, for the  $\ell_{4/3}$ -norm sparsity constraint  $\|Y\|_{4/3} \leq \gamma$ ,  $\gamma$  should take value from the interval  $(1, (pk)^{4/3})$  (Figure 3 right panel).

Our simulation shows that the SMA is robust to a wide span of parameter settings (Section 5.2). For example, we observed that setting  $\gamma = \sqrt{pk}$  in SCA (or  $\gamma_z = \sqrt{nk}$  and  $\gamma_y = \sqrt{pk}$  in SMA) generally yields meaningful sparse estimates. Hence, we set this as the default value for  $\gamma$ . The sparsity parameter can also be selected based on the data. For completeness, we describe a cross-validation schema for selecting parameters in Appendix C.

### 3.3 Rotation: Varimax and Absmin

In this section, we discuss two orthogonal rotation techniques, the varimax rotation and the newly devised *absmin* rotation. The two rotation methods are motivated to introduce sparse structure and are derived from the  $\ell_{4/3}$ -norm and  $\ell_1$ -norm penalty functions respectively. The  $\ell_{4/3}$ -norm penalty is a smooth approximation to  $\ell_1$  that also promotes sparse structure.

For any  $A \in \mathbb{R}^{p \times k}$ , the *varimax criterion* is defined as the sum of column (sample) variance of squared values ( $A_{ij}^2$ ) (Kaiser, 1958):

$$C_{\text{varimax}}(A) = \sum_{j=1}^k \left[ \frac{1}{p} \sum_{i=1}^p A_{ij}^4 - \frac{1}{p^2} \left( \sum_{i=1}^p A_{ij}^2 \right)^2 \right].$$

For a fixed  $Y$ , the *varimax rotation* seeks an orthogonal rotation  $R$  to maximize the varimax criterion on rotated matrix  $YR$ ,

$$\underset{R}{\text{maximize}} \quad C_{\text{varimax}}(YR) \quad \text{subject to } R \in \mathcal{U}(k). \tag{12}$$

4. Condition  $\gamma > k$  is not necessary for the maximization of (5) or (11), because of the  $\ell_2$ -norm inequality constraints,  $Y \in \mathcal{B}(p, k)$ .

It is commonly applied in factor analysis for producing nearly sparse and easily interpretable loadings of PCs, especially in psychology literature. The varimax rotation is easy to compute; for example, the base function `varimax` in the R implements a gradient projection algorithm for it (Bernaards and Jennrich, 2005). Jennrich (2001) showed that the gradient projection algorithm converges to a local minima globally from any starting point and enjoys geometric (or linear) convergence rate.

In our application to SCA (and SMA), where  $Y \in \mathcal{V}(p, k)$ , the varimax criterion naturally links to the  $\ell_{4/3}$ -norm objective function in (9). In particular, since the columns of  $Y$  have unit length,  $\sum_{i=1}^p Y_{ij}^2 = 1$ , the varimax criterion reduces to a simpler form (also known as the *quartimax* criterion as introduced in Carroll (1953)) up to a constant:

$$C_{\text{quartimax}}(Y) = \sum_{i=1}^p \sum_{j=1}^k Y_{ij}^4. \quad (13)$$

This equals the  $\ell_4$ -norm of  $Y$  to the power of 4. Since  $\|Y\|_F = \sqrt{k}$ , Hölder's inequality says that (using the Hölder conjugates  $4/3$  and  $4$ )

$$\|Y\|_{4/3} \geq \frac{\sqrt{k}}{\|Y\|_4}.$$

This implies that maximizing the varimax criterion is the dual problem of minimizing the  $\ell_{4/3}$ -norm objective. Hence, to update  $Y$  in the algorithm of SCA, we invoke the varimax rotation in (12) as a proxy for (9).

As for the  $\ell_1$ -norm penalty (lasso), we define the *absmin* rotation that minimizes the sum of absolute values of the rotated matrix,

$$\underset{R}{\text{minimize}} \quad \sum_{i=1}^p \sum_{j=1}^k |[YR]_{ij}| \quad \text{subject to } R \in \mathcal{U}(k), \quad (14)$$

where  $Y \in \mathbb{R}^{p \times k}$  is given and fixed. The objective function in (14) is smooth almost everywhere; the only non-smooth points are those  $YR$  that contain at least one zero. Consider again the application to the Stiefel manifold, e.g.,  $Y \in \mathcal{V}(p, k)$ . For some  $R \in \mathcal{U}(k)$ , suppose the objective in (14) is differentiable at  $YR$  (i.e.,  $[YR]_{ij} \neq 0$  for all  $i$  and  $j$ ). Then, the gradient direction of this objective function at  $R$  takes a simple form,  $Y^T \text{sign}(YR)$ , where  $\text{sign}(\cdot)$  is the element-wise sign function. This suggests a projected gradient algorithm to compute the absmin rotation (Bernaards and Jennrich, 2005). In our numerical experiments and data applications, the absmin rotation performs similarly to the varimax rotation. Hence, for simplicity, we focus on the varimax rotation in Algorithm (1). However, the varimax rotation could be replaced by any other rotation technique. There are a wide array of them in the factor analysis literature and in the literature on ICA.

### 3.4 Shrinkage: Soft-thresholding

In the PRS update (Algorithm 1), the last step projects the rotated matrices (i.e.,  $Y^*$  and  $Z^*$ ) onto the feasible set with a shrinkage operator. In particular, soft-thresholding is chosen for the  $\ell_1$ -norm penalty. Consider an orthogonal design case where  $Z^T X$  has orthogonal columns. Let  $Y \in \mathcal{V}(p, k)$  and  $\hat{Y} \in \mathcal{B}(p, k)$  be two matrices before and after a shrinkage operation respectively. Then, the decreasing of the objective value in (5) or (11) caused by the shrinkage is easily shown upper bounded by  $\|\hat{Y} - Y\|_F$ . It follows that soft-thresholding is the “best” shrinkage that minimizes this

upper bound for the  $\ell_1$ -norm constraint. Here, the soft-thresholding with a sparsity parameter  $\gamma$  is defined element-wisely for  $A \in \mathbb{R}^{p \times k}$  as (Donoho, 1995)

$$[T_\gamma(A)]_{ij} = \text{sign}(A_{ij}) \cdot (|A_{ij}| - t)_+, \quad (15)$$

where  $x_+$  is defined to equal  $x$  if  $x > 0$  and 0 otherwise, and  $t > 0$  is the threshold determined by the equation  $\|T_\gamma(A)\|_1 = \gamma$ , where  $\gamma$  is the sparsity parameter.

Soft-thresholding is widely used for creating sparse structure (e.g., Tibshirani, 1996). It is also easy to implement given the sparsity parameter. The cut-off value  $t$  in (15) can be quickly found with a binary search in logarithmic time,  $\mathcal{O}(-\log_2(\varepsilon))$ , where  $\varepsilon$  is the convergence tolerance. In addition, soft-thresholding can preserve a large amount of the PVE and maintain to some degree the orthogonality, if the cut-off value  $t$  is sufficiently small (see Appendix D for details).

## 4. Sparse PCA Performs Independent Component Analysis

In this section, we demonstrate the connection between sparse PCA (specifically, our SCA formulation) and ICA.

### 4.1 Independent Component Analysis

ICA is motivated by blind-source (or blind-signal) separation in signal processing (see, e.g., Comon and Jutten, 2010), where we observe a series of multivariate signals  $X_i \in \mathbb{R}^p$  for  $i = 1, 2, \dots, n$ , where  $n$  is the number of observations. In ICA, there exist  $k$  independent, non-Gaussian and unobserved *source* signals underlying each observation,  $Z_i \in \mathbb{R}^k$  for  $i = 1, 2, \dots, n$ , and each observation is a linear mixture of these source signals, this is,  $X = ZM^T$  (or  $X_i = Z_i.M$  for  $i = 1, 2, \dots, n$ ), where  $M \in \mathbb{R}^{p \times k}$  is the *mixing* matrix. ICA aims to “un-mix” the observed  $X$  and extract  $Z$  from it. In particular, since the  $k$  source signals are independent, it is often assumed that  $Z$ ’s columns have unit length and are orthogonal to each other (i.e.,  $Z \in \mathcal{V}(n, k)$ ). The ICA literature is rich in theoretical results (Hyvärinen and Oja, 2000; Chen and Bickel, 2006; Samworth and Yuan, 2012; Miettinen et al., 2015), and most methods for ICA (e.g. fastICA) identifies both sparse and non-sparse source signals.

We consider a sparse version of ICA, sparse ICA, where  $Z$  is sparse (or the columns of  $Z$  follow leptokurtic distributions). We show that sparse ICA and sparse PCA are unified by the SMA. To see this, recall from Section 2.2 that the SMA of a data matrix is  $ZBY^T$ , where  $Z$  and  $Y$  are both sparse but  $B$ . We interpret the SMA for the two modern multivariate data analysis:

**Sparse PCA** For sparse PCA, we treat  $Y$  as the sparse loadings, and  $ZB$  together as the component scores.

**Sparse ICA** For sparse ICA, the sparse source signals (or the independent components) are the columns of  $Z$ , the mixing matrix is  $BY^T$ .

It can be seen that both sparse PCA and sparse ICA seek a sparse component in the data: sparse PCA extracts them for the column space ( $Y$ ), while ICA the row space ( $Z$ ). Hence, performing sparse PCA to the transposed input data matrix actually accomplishes sparse ICA to the original data. This highlights the similarities between sparse PCA and sparse ICA.

## 4.2 Algorithmic Similarity and Assumptive Nuances

Another insight for sparse PCA and sparse ICA can be gleaned from their algorithms. In this section, we demonstrate that the fastICA algorithm (Hyvarinen, 1999) and our SCA algorithm are both closely related to kurtosis (Mardia, 1970).

The fastICA algorithm finds  $Z$  in two steps. The first step is to pre-process  $X$ . The pre-processing of centering and whitening (see, e.g., Comon (1994)) results in the leading  $k$  left singular vectors  $\hat{U} \in \mathcal{V}(n, k)$ . The second steps searches for an orthogonal rotation that maximize the non-gaussianity of  $\hat{U}R$ , as measured by the approximation of negentropy,

$$\underset{R}{\text{maximize}} \quad \sum_{j=1}^k \{ \mathbb{E} G([UR]_{\cdot j}) - \mathbb{E} G(v) \}^2 \quad \text{subject to } R \in \mathcal{U}(k), \quad (16)$$

where  $G(x)$  is a non-quadratic function for  $x \in \mathbb{R}^n$ , and  $v \sim \mathcal{N}(0, I_n)$  is the multivariate standard Gaussian vector. Finally,  $\hat{U}\hat{R}$  is the fastICA estimate for  $Z$ , where  $\hat{R}$  is the solution to (16). Hyvarinen (1999) noted that setting  $\mathbb{E} G(x) = \|x\|_4^4/n$ , the optimization in (16) takes the form<sup>5</sup>

$$\underset{R}{\text{maximize}} \quad \sum_{j=1}^k \text{kurt}^2([UR]_{\cdot j}) \quad \text{subject to } R \in \mathcal{U}(k), \quad (17)$$

where  $\text{kurt}(x)$  is the sample excess kurtosis of  $x \in \mathbb{R}^n$  and is defined as  $\text{kurt}(x) = n \sum_{i=1}^n (x_i - \bar{x})^4 / (\sum_{i=1}^n (x_i - \bar{x})^2)^2 - 3$ , where  $\bar{x} = \sum_{i=1}^n x_i/n$  is the mean. It can be seen from (17) that fastICA produces either leptokurtic ( $\text{kurt}(x) > 0$ ) or platykurtic ( $\text{kurt}(x) < 0$ ) estimation for the columns of  $Z$ , because of the squared kurtosis in the objective function. This primarily explains that fastICA allows both sparse and non-sparse source signal, recognizing that any sparse distribution is leptokurtic (see Theorem 2.1 of Rohe and Zeng (2020)).

As for SCA, the algorithm uses the varimax rotation to find the orthogonal rotation. Suppose  $Y \in \mathcal{V}(n, k)$ . Since the sum of squares of  $Y$ 's columns are constant,  $\sum_{j=1}^k Y_{ij}^2 = 1$ , maximizing the varimax rotation is equivalent to maximizing the sum of sample kurtosis of  $Y$ 's columns,

$$C_{\text{varimax}}(Y) = \sum_{j=1}^k \text{kurt}(Y_{\cdot j}) + \text{constant}.$$

This suggests that the varimax rotation in SCA promotes some leptokurtic columns in the loading  $Y$  of sparse PCs. Hence, ICA corresponds to simultaneously maximizing and minimizing the varimax criterion in (12).

SCA aims to identify sparse PCs, while ICA focuses on finding independent components that may be sparse or non-sparse. If the source signals are presumed sparse, then the two analysis are expected to perform similarly on the transposed data matrix. However, there are a few assumptions for sparse PCA and ICA that differ. In many applications of ICA, the number of independent components and the number of observed variables are the same (i.e.,  $p = k$ ), in which case, the mixing matrix is square. The  $p = k$  regime is generally challenging. As such, many theoretical results presume no or very little noise in  $X$ , in order for estimating guarantees. By contrast, sparse PCA typically presumes the data to comprise noise and the statistical model usually contain a noise term. In addition, it is showed that sparse PCA is consistent even when the observed data is high-dimensional (i.e.,  $p$  grows at the same rate as  $n$ ) or sparse by itself (i.e. contains many zeros) (Rohe and Zeng, 2020), while it is unclear yet whether ICA is consistent or not under these settings.

---

5. The authors also suggested different forms of  $\mathbb{E} G(x)$ .



## 5. Simulation Studies

We conducted simulation studies to compare sparse PCA methods. Specifically, we focused on their power of explaining the variance in data, the robustness under various sparsity levels, and the computational efficiency. For comparisons, we selected SPCA, SPC, GPower, the SPCAvRP method recently proposed by Gataric et al. (2020), SCA, and another variant of SCA which deploys the absmin rotation (SCA-absmin). For SCA and SCA-absmin, we implemented the algorithms in R.<sup>6</sup> For SPCA, SPC, and SPCAvRP, we invoked the R packages `elasticnet`, `PMA`, and `SPCAvRP` respectively. The implementation of GPower (in MATLAB) was obtained from the authors’ website. For all the all iterative methods, we specified maximum number of iteration to 1,000 for and the stopping (convergence) criterion to  $10^{-5}$  if applicable. Overall, our numerical experiments showed that the SCA algorithm converges quickly and produces robust and sparse PCs that capture a large amount of variance in the data.

### 5.1 Proportion of Variance Explained

In this simulation study, we compared the six sparse PCA methods by their abilities of explaining the variance in the data. To this end, we simulated 30 data matrices with  $n = 100$  observations and  $p = 100$  variables from the following low-rank generative model:

$$X = SY^T + E,$$

where  $S \in \mathbb{R}^{100 \times 16}$  contains the component scores, and  $Y \in \mathbb{R}^{100 \times 16}$  contains the loadings of sparse PCs, and  $E \in \mathbb{R}^{100 \times 100}$  is some noise. We generated the scores  $S$  using a low-rank SVD approach—first, we randomly sampled  $U$  from  $\mathcal{V}(100, 16)$  and  $V$  from  $\mathcal{U}(16)$ , then we set  $S = U\Sigma V^T$ , where  $\Sigma$  is a diagonal matrix with the diagonals  $\sigma_i = 10 - \sqrt{i}$  for  $i = 1, 2, \dots, 16$ . To simulate the sparse loadings  $Y$ , we first sampled a  $100 \times 16$  matrix from  $\mathcal{V}(100, 16)$ , then soft-threshold its elements with the function  $T_{20}$  (as defined in Equation (15)). Note that, it is unnecessary to re-scale the columns of loadings to unit length, because  $S$ ’s columns can absorb these scalars. Lastly, the elements in  $E$  were sampled independently from the normal distribution,  $E_{ij} \sim N(0, 0.1^2)$ .

We applied the six sparse PCA methods on each simulated data matrix  $X$  to compute  $k = 2, 4, 6, \dots, 16$  sparse PCs. For each  $k$ , we configured the same  $\ell_1$  norm of the returned loadings across different methods. Specifically, for SCA, SCA-absmin, and SPC, we directly constrained the  $\ell_1$  norm of sparse loadings to  $2.5k$  (i.e., 2.5 per PC on average). As for SPCA, GPower and SPCAvRP, we tuned the parameters such that the returned loadings all have the same  $\ell_1$  norm of  $2.5k$ . As a result, we calculated the PVE (as defined in Section 3.1) for each method. Note that the PVE by sparse PCs is upper bounded by that of traditional PCs (no sparsity constraint), therefore, we also applied traditional PCA and treated it as a “gold standard.” Figure 4a displays the mean PVE for traditional PCA and the six sparse PCA methods, with the requested number of PCs varying from 2 to 16. It can be seen that SPCAvRP and SPCA explained less than half of the variance in the data, and that GPower and SPC both exhibited improved performance over SPCA. For GPower, we tested both the single-unit and the block version, but the block version often converged to a defective solution with some columns decaying to all zeros. This happened when the number of targeted PCs went above 5 in this simulation. Overall, SCA and SCA-absmin performed better than the other methods and the

6. We provide an R package `epca`, for **e**xploratory **p**roduct **p**roject **a**nalysis, which implements SCA and SMA with various algorithmic options. The package is available from CRAN (<https://CRAN.R-project.org/package=epca>).

closest to traditional PCA. In addition, the SCA algorithm converged with fewer iterations than the other sparse PCA methods (see Table 1 for a comparison when  $k = 16$ ). It is also shown in the table that SCA was more computationally efficient than SCA-absmin, due to the absmin rotation.

Method	# of iterations	Mean run time (s)	Environment
SCA	10 ~ 65 (all the PCs)	0.96	R
SPC	25 ~ 1,000 (each PC)	1.21	R
GPower	30 ~ 150 (each PC)	0.19	MATLAB
SPCA	470 ~ 920 (all the PCs)	56.30	R
SPCAvRP	/	28.67	R
SCA-absmin	/	23.5	R

Table 1: Comparison of the computational efficiency of sparse PCA methods. Each method is tasked to find 16 PCs using a single processor (2.50GHz). SPCAvRPs is not iterative (yet is parallelizable), hence the number of iterations is not applicable. The absmin rotation is less efficient, so we halted the algorithm of SCA-absmin after the 15th iteration.

## 5.2 Robustness against Tuning Parameters

This simulation study investigates the robustness of sparse PCA methods against the changes in the sparsity parameter. For this, we chose to apply sparse PCA to community detection in networks (or graph partitioning) (see, e.g., Fortunato, 2010), using the graph adjacency matrix (see the definition below) as the input. This is motivated by the recent results in Rohe and Zeng (2020) showing that under the stochastic block model (SBM, see for example Holland et al., 1983), each sparse PC of the adjacency matrix estimates an indicator of the community memberships.

We simulated 30 undirected graphs with  $n = 900$  nodes and four equally sized blocks from the SBM. Under the SBM, the edge between node  $i$  and  $j$  is sampled from the Bernoulli distribution,  $\text{Bernoulli}(B_{z(i),z(j)})$ , where  $z(i) \in \{1, 2, 3, 4\}$  is the membership of node  $i$ , and

$$B = 0.05 \times \begin{bmatrix} 0.6 & 0.2 & 0.1 & 0.1 \\ 0.2 & 0.7 & 0.05 & 0.05 \\ 0.1 & 0.05 & 0.6 & 0.25 \\ 0.1 & 0.05 & 0.25 & 0.6 \end{bmatrix}$$

is the block connectivity matrix. Under this setting, the expected number of edges connected to each node is 45. For each simulated graph, we defined the adjacency matrix  $A \in \{0, 1\}^{n \times n}$  with  $A_{ij} = 1$  if  $i$  and  $j$  are connected and 0 otherwise.

We applied SCA, SPC, and GPower on each of the 30 simulated adjacency matrices to estimate four sparse PCs—since SPCA and SPCAvRP performs worse than SPC and GPower (Zou and Xue, 2018), we excluded the two in this simulation for simplicity—with varied sparsity parameter. For SCA, we imposed that  $\|Y\|_1 \leq \gamma$ , and for SPC, we imposed on each column  $y_j$  that  $\|y_j\|_1 \leq \gamma/4$ , with  $\gamma \in \{18, 24, 36, 48, 60, 66\}$ . As for GPower, we tuned the parameters such that the returned loadings have the same  $\ell_1$  norm. Figure 4b depicts, for example, the estimated loadings returned by SCA and SPC on one of the adjacency matrices. It can be seen that the supports of the four PCs separate the nodes by their block memberships. As such, we used the sparse loadings to cluster

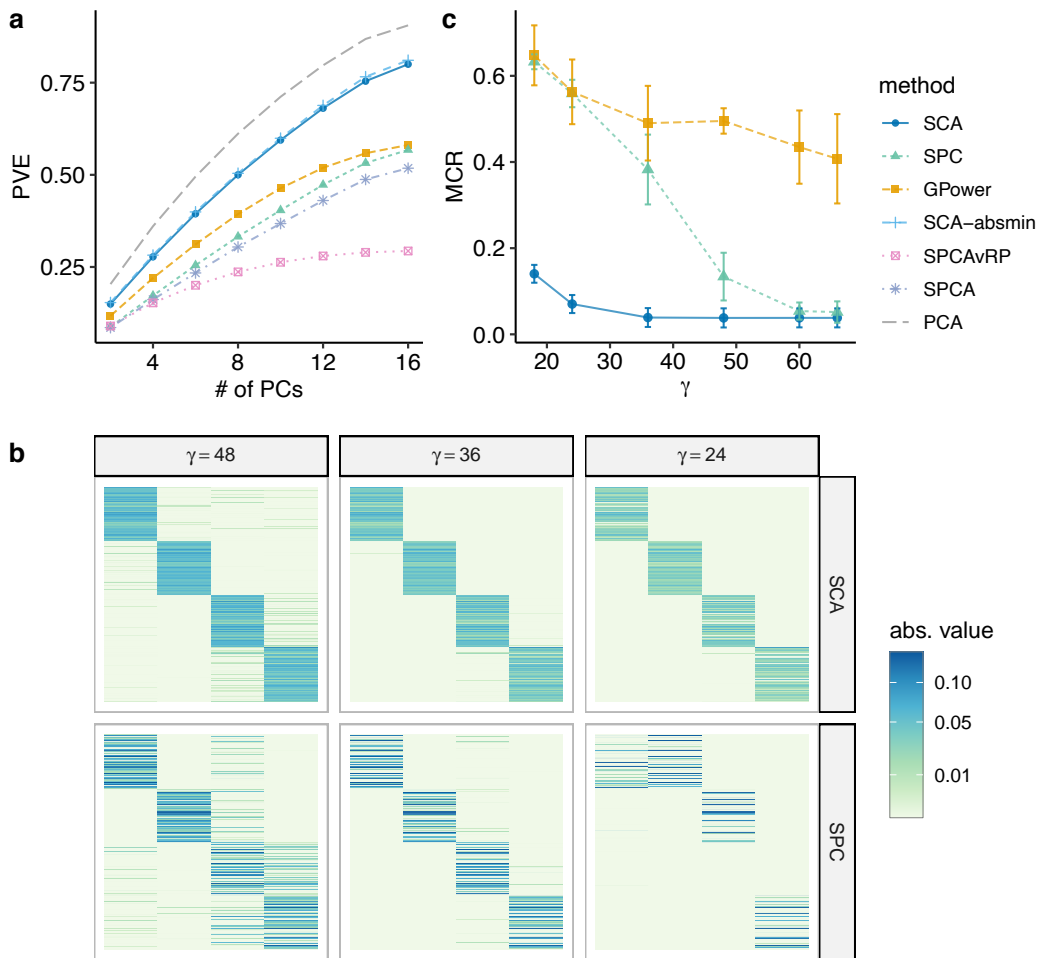


Figure 4: Comparisons of sparse PCA methods using simulated data. (a) The proportion of variance explained (PVE) by the (sparse) principal components (PCs) returned by SCA (blue circles), SCA-absmin (cyan plus signs), GPower (yellow squares, the single-unit version), SPC (green triangles), SPCA (purple asterisks), SPCAvRP (pink boxes), and traditional PCA (grey), with the number of targeted PCs varying from 2 to 16. (b) Heat maps of the sparse PC loadings returned by SCA and SPC, with three different sparsity parameters ( $\gamma = 24, 36, 48$ ). In each heat map, each row corresponds to one node, ordered by the true community membership, and each of the four columns corresponds to one sparse PC. The color shade indicates the absolute value of the estimated loading. (c) The mis-classification rate (MCR) of community detection returned by SCA, GPower, and SPC, with varied sparsity parameters ( $\gamma$ ). Each point indicates the mean MSR across 30 replicates of networks. For each point, an error bar indicates the three times of standard deviation.

nodes and assessed the quality of the sparse PCA methods by the quality of the clustering. To this end, we assigned node  $i$  to cluster  $j$  if  $Y_{ij}$  is the largest absolute value in row  $i$ , that is  $|Y_{ij}| > |Y_{il}|$  for all  $l \neq j$ . In case of ties or for a row of zeros, the cluster label is randomly assigned. For each estimate, let  $C \in \{1, 2, 3, 4\}^n$  be the assigned cluster labels and  $C^* \in \{1, 2, 3, 4\}^n$  be the true label, we define the mis-classification rate (MCR) as (Qin and Rohe, 2013)

$$\text{MCR}(C, C^*) = \frac{1}{n} \sum_{i=1}^n \mathbb{1}(C_i \neq C_i^*).$$

Figure 4c summarizes the MCR for the three methods using different sparsity parameters. It can be seen that the performance of GPower and SCA were less affected by the change in sparsity parameter, while SPC was profoundly influenced by such change. As  $\gamma$  became smaller, SPC lost the identification of for clusters faster, suggesting that SPC is more sensitive to the choices of tuning parameter. Although less sensitive to the change in  $\gamma$ , GPower produced poor estimation of sparse PCs, with the MCR only slightly better than random guess (whose  $\text{MCR} = 0.75$ ). Overall, SCA exhibited lower MCR with smaller deviation compared to the others, suggesting that SCA is more robust to the choices of the sparsity parameter.

## 6. Applications

In this section, we first demonstrate the utility of sparse PCA as sparse ICA with an image coding application, which is considered widely in the ICA literature. Appendix E contains an additional application of SCA to blind source separation of images. Next, we demonstrate the efficacy of SCA and SMA with applications to a transcriptome sequencing data set and a targeted sample of Twitter friendship network.

### 6.1 Sparse Coding of Images

Low-level visual layers, such as retina, the lateral geniculate nucleus, and the primary visual cortex (V1) are shared processing components in mammalian. The receptive fields in the V1 can be characterized as being spatially localized, oriented and bandpass (i.e., selective to structure at different spatial scales). To understand V1, one line of research focuses on finding sparse and linearly independent codes for natural images, which provides an efficient representation for later stages of processing (Field, 1994; Olshausen and Field, 1996; Bell and Sejnowski, 1997). This type of research is based on the hypothesis of sparse coding, that is, any perceived scenes can be synthesized via the linear combination of some small subsets of basis images (Lee et al., 2006; Gregor and LeCun, 2010)). In this application, we show that sparse PCA produces a set of bases for natural images that resembles those found in Olshausen and Field (1996).

We utilized ten natural images from Olshausen and Field (1996), each of pixel size  $512 \times 512$ , and followed the same whitening process as described by the authors. Next, we randomly sampled a total of 12,000 small image patches of size  $16 \times 16$  from the ten images, followed with a centering step (i.e., subtract each pixel by the mean of all 256 pixels). We vectorized each patch of image and put them into the rows of a data matrix,  $X \in \mathbb{R}^{n \times p}$ , where  $n = 12,000$  and  $p = 256$ . We inputted the transposed matrix,  $X^T$ , to SCA and look for 49 sparse PCs ( $k = 49$ ) with the default sparsity parameter,  $\gamma = \sqrt{pk}$ . In particular, for the varimax rotation, we normalized the rows to unit length scaled back afterward, as recommended by Kaiser (1958). In the output of SCA, the estimated scores

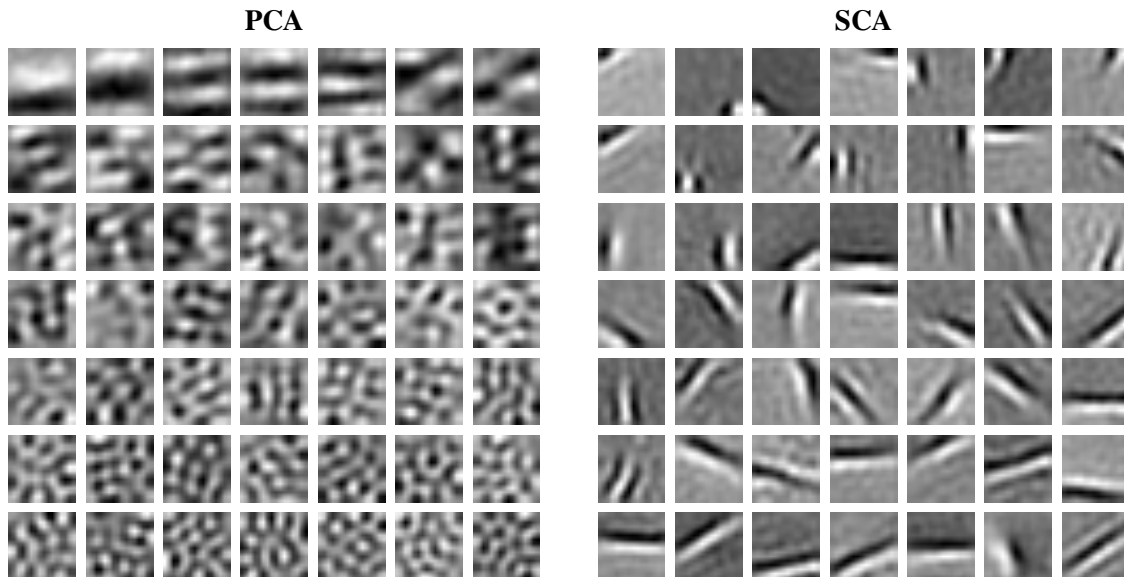


Figure 5: Sparse image encoding using traditional PCA (left) and sparse PCA (right). For both method, shown are the 49 image bases (i.e., component scores) extracted from natural images. Each image basis is in  $16 \times 16$  pixel.

$S \in \mathbb{R}^{p \times k}$  contains the basis images, and the estimated sparse loadings  $Y \in \mathbb{R}^{n \times k}$  encodes how the basis images are linearly combined for each image patch (i.e.,  $Y$  contains the linear coefficients). We note that this is sparse coding.

Figure 5 displays the 49 image bases returned by PCA and SCA, where each image represents one column of  $S$  as transformed into a  $16 \times 16$  array. For SCA, it can be seen that the basis images produced exhibit some basic graphical patterns such as lines and edges. As for PCA, the oriented structure in the first few basis images does not arise as a result of the oriented structures in natural images, yet more likely because of the existence of those components with low spatial frequency (Field, 1987). This application validates that sparse PCA can perform ICA in identifying sparse source signals and suggests that sparse PCA has potentially broader usefulness in image processing.

## 6.2 Analysis of Single-cell Gene Expression

Single-cell transcriptome sequencing (scRNA-seq) provides the genome-wide expression profiles of individual cells. It has been widely used across biological disciplines. For example, patterns of gene expression can be identified through clustering analysis. This can uncover the existence of rare cell types within a cell population that have never been seen (Plasschaert et al., 2018; Montoro et al., 2018). In this application, we aimed to use SCA to extract the sparse PCs of genes from scRNA-seq data that characterize the known cell types.

For this application, we used the human pancreatic islet cell data from Baron et al. (2016). We removed the genes that do not have any variation across samples (i.e., zero standard deviation) and the cell types that contain fewer than 100 cells. This resulted in a data matrix  $X \in \mathbb{R}^{n \times p}$  of  $p = 17499$  genes and  $n = 8451$  cells across nine cell types, where  $X_{ij}$  is the expression level of gene  $j$  in cell

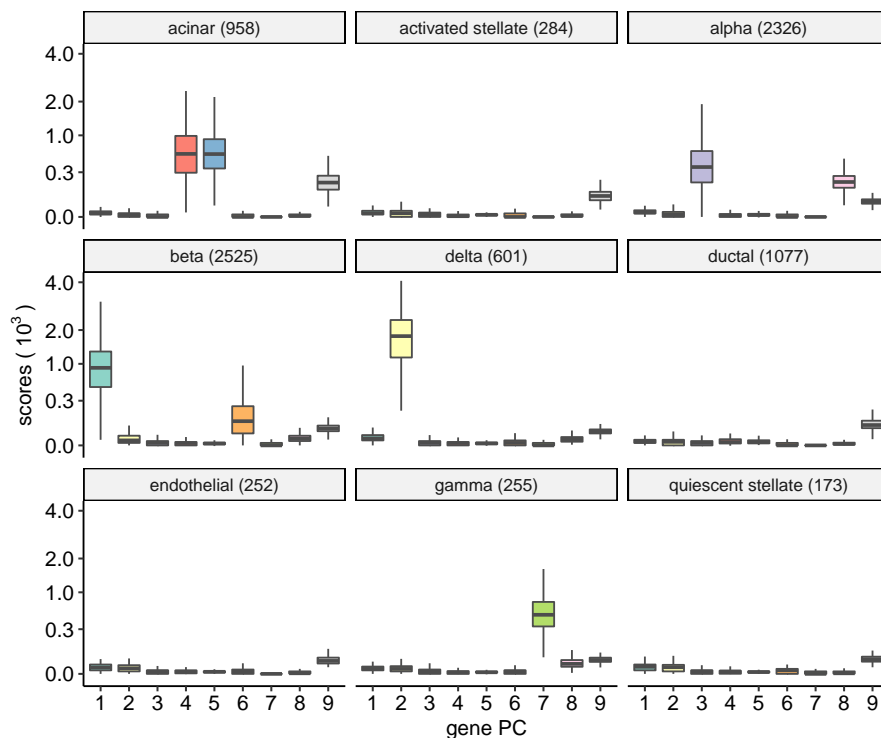


Figure 6: Scores of sparse gene principal components (PCs) stratified by cell types. Each panel displays one of nine cell types with the names of cell types and the number of cells reported on the top strips. For each cell type, a box depicts the component scores for nine sparse gene PCs.

PC	# of genes	Gene name(s)
1	1	INS
2	1	SST
3	1	GCG
4	8	CTRB2, REG1A, REG1B, REG3A, SPINK1 ...
5	15	CELA3A, CPA1, CTRB1, PRSS1, PRSS2 ...
6	1	IAPP
7	1	PPY
8	3	CLU, GNAS, TTR
9	61	ACTG1, EEF1A1, FTH1, FTL, TMSB4X ...

Table 2: Sparse gene PCs estimated by SCA. For each gene PC, the number of genes (i.e., the number of non-zeros in the loadings) and the top 5 genes according to the absolute loadings are reported.

$i$ , with 10.8% being non-zero. We applied SCA on  $X$  for  $k = 9$  sparse gene PCs. Aiming for a small number of genes (i.e., non-zero loadings) in individual PCs, we set the sparsity parameter to  $\gamma = \log(pk) \approx 12$ . The algorithm took 24 iterations and about 5 minutes on a single processor (3.3GHz). As a result, Figure 6 displays the component scores of the nine PCs. We observed that most of the gene PCs consist of one or a handful of genes, yet the component scores showed that these PCs distinguish different cell types effectively (Table 2). For example, the PC 2 consists of only one gene (SST), and the expression of the gene marks the “delta” cells among others. This result highlights power of scRNA-seq in capture cell-type specific information and suggests the applicability of our methods to biological data.

### 6.3 Clustering of Twitter

This application serves in our grand efforts to study political communication using the social network, Twitter. Twitter is organized so that users primarily read the tweets from their friends that they “follow”. Each user can freely decide who to follow (and “unfollow”) in order to select the content that they want to consume. As such, the communication on Twitter can be contextualized by the friendship network, which offers more insights into the expression of public opinion on social media. In this section, we demonstrate our methods with a large-scale clustering of Twitter accounts that was used to develop the website [www.murmuration.wisc.edu](http://www.murmuration.wisc.edu) (Zhang et al., 2020). For this application, we used a targeted sample of the Twitter friendship network collected in August 2018 (Chen et al., 2020). In this sample, there are  $n = 193,120$  Twitter accounts who follow a total of  $p = 1,310,051$  accounts, after filtering out accounts with few followers or followings. We defined the graph adjacency matrix  $A \in \{0, 1\}^{n \times p}$  with  $A_{ij} = 1$  if and only if account  $i$  follows account  $j$ .<sup>7</sup> This resulted in a sparse  $A$  with about 0.02% entries being 1.

Zhang et al. (2020) applied a two-way analysis to find  $k = 100$  clusters of Twitter accounts in the rows and columns of  $A$ . Figure 2 displays seven PC loadings for 1500 randomly selected Twitter accounts in the columns of  $A$ . This analysis was computationally tractable; one iteration of the SMA algorithm took about 54 minutes on a single processor (2.5GHz), thanks to the efficient algorithm that computes the sparse SVD (Baglama and Reichel, 2005). Then, the clusters of Twitter accounts were determined as follows (same as in Section 5.2): the  $i$ th row account of  $A$  was assigned to the  $l$ th row cluster if  $Z_{il}$  was the greatest in the  $i$ th row of  $Z$ , that is,  $|Z_{il}| \geq |Z_{il'}|$  for all  $l' = 1, 2, \dots, k$ , and the  $j$ th column account of  $A$  was assigned to the  $l$ th column cluster if  $Y_{jl}$  was the greatest in the  $j$ th row of  $Y$ ,  $|Y_{jl}| \geq |Y_{jl'}|$  for all  $l' = 1, 2, \dots, k$ . As a result, it was observed that the clusters of Twitter accounts formed homogeneous, connected, and stable social groups (Zhang et al., 2020). Furthermore, the estimated row clusters and column clusters are matched (Rohe et al., 2016), that is, the  $k$ th row cluster tends to follow the accounts in the  $k$ th column cluster. To illustrate this, we quantified the number of followings from the row clusters to the corresponding column clusters. Figure 7 displays the results for 50 selected clusters that are related to U.S. politics. It can be seen that the number of followings between each paired row and column clusters (i.e., the diagonal) showed marked enrichment. These results suggest the efficacy of our methods for social media data analysis.

---

7. The columns of  $A$  are not centered nor scaled. One alternative is to normalize and regularize the adjacency matrix as  $L \in \mathbb{R}^{n \times p}$  with  $L_{ij} = A_{ij} / \sqrt{(r_i + \bar{r})(c_j + \bar{c})}$ , where  $r_i = \sum_j A_{ij}$  is the sum of the  $i$ th row of  $A$ ,  $c_j = \sum_i A_{ij}$  is the sum of the  $j$ th column of  $A$ , and  $\bar{r}, \bar{c}$  are their means (Zhang and Rohe, 2018).

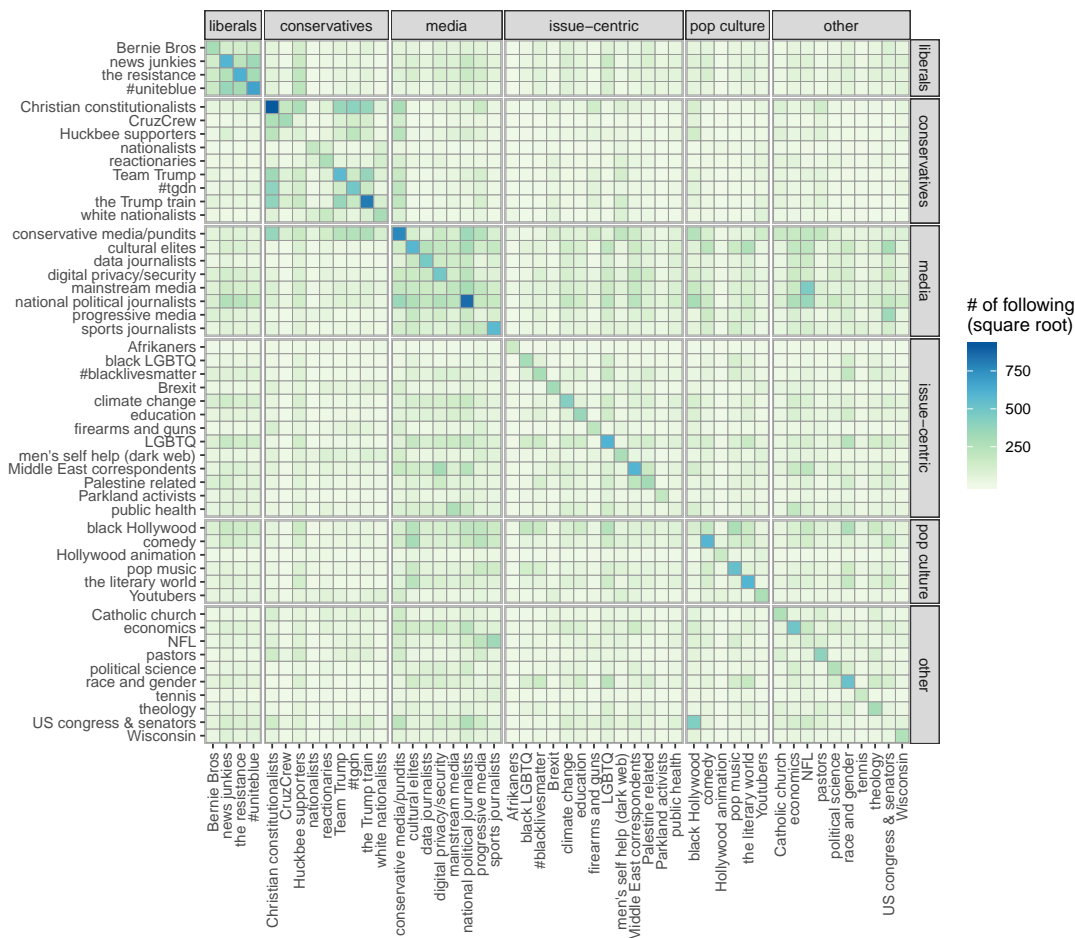


Figure 7: Heat map of friend counts between row and column clusters of Twitter accounts. Each row and column corresponds to a cluster. The row and column panels indicate cluster category, with the category names shown in the top and right strips. The color shades indicate the number of followings from the row cluster to the column cluster, after the square root transformation.

## 7. Discussions

In this paper, we introduce SCA, a new method for sparse PCA, and its extension, the SMA, for two-way data analysis. SCA differs from previous sparse PCA methods because it considers a new (orthogonally rotated) basis for PCs. This is particularly useful when a data matrix is presumed low-rank but its singular vectors (or the eigenvector of the covariance matrix) are not readily sparse, as often happens in realistic data analysis (e.g., Figure 2). The proposed sparse PCA algorithm (Algorithm 2) explains more variation in the data compared to the state-of-the-art methods, especially when multiple PCs are desired (e.g.,  $k \geq 4$ ), and it does so without the need for deflation. Furthermore, the algorithm is stable and robust against the choices of tuning parameter.



## Acknowledgments

This research is partially supported by National Science Foundation grant DMS-1612456 and DMS-1916378 and Army Research Office grant W911NF-15-1-0423. We thank Sündüz Keleş, Sébastien Roch, Po-Ling Loh, Michael A Newton, Yini Zhang, Muzhe Zeng, Alex Hayes, E Auden Krauska, Jocelyn Ostrowski, Daniel Conn, and Shan Lu for all the helpful discussions.

## Appendices

### A. Technical Proofs

**Proof of Proposition 1** We show that for any fixed  $Z$  and  $Y$ , the inequality holds for the minimization over  $B$  on the left-hand-side and the diagonal  $D$  on the right-hand-side,

$$\min_B \|X - ZBY^T\|_F^2 \leq \min_D \|X - ZDY^T\|_F^2.$$

In fact, the maximizer of the left-hand-side is  $B^* = (Z^T Z)^{-1} Z^T X Y (Y^T Y)^{-1}$  if  $Z$  and  $Y$  are full-rank, or  $B^* = (Z^T Z)^+ Z^T X Y (Y^T Y)^+$  if either  $Z$  or  $Y$  is singular, where  $A^+$  is the Moore–Penrose inverse of matrix  $A$ . Since  $B^*$  is not diagonal in general, the inequality follows. ■

**Proof of Lemma 2** We rewrite the objective function:

$$\begin{aligned} \|X - ZBY^T\|_F^2 &= \text{tr} \left[ (X - ZBY^T)^T (X - ZBY^T) \right] \\ &= \|X\|_F^2 - 2 \text{tr} \left( X^T ZBY^T \right) + \text{tr} \left( B^T B \right) \\ &= \|X\|_F^2 - \text{tr} \left[ B^T \left( 2Z^T XY - B \right) \right]. \end{aligned}$$

For fixed  $Z$  and  $Y$ , take the derivative of  $B$  and set it to zero. We have the optimizer  $B^* = Z^T XY$  and the squared optimal value is  $\|X\|_F^2 - \|Z^T XY\|_F^2$ . Recognizing that  $\|X\|_F^2$  is determined, the desired formulation (11) follows. ■

**Remark 4 (Minimal matrix reconstruction error of PMD)** *If  $B$  is constrained to a diagonal matrix in (10), then the squared minimal value is*

$$\|X\|_F^2 - \sum_{i=1}^k d_i^2 \quad \text{where} \quad d_i = [Z^T XY]_{ii}, i = 1, 2, \dots, k.$$

**Proof** From the proof of Lemma 2, we have

$$\|X - ZDY^T\|_F^2 = \|X\|_F^2 - \text{tr} \left[ D^T \left( 2Z^T XY - D \right) \right].$$

Then, take the derivative of  $D$  and set it to zero. This yields the solution  $\hat{D} = \text{diag}(d_i)$ , where  $d_i = [U^T X V]_{ii}$ . Finally, plugging-in the maximizer  $\hat{D}$  gives the claimed optimal value. Note that

$$\sum_{i=1}^k d_i^2 \leq \|U^T X V\|_F^2. \quad \blacksquare$$

**Proof of Lemma 3** Suppose the low-rank SVD of  $C \in \mathbb{R}^{p \times k}$  is  $UDV^T$ , where  $U \in \mathcal{V}(p, k)$ , and  $V \in \mathcal{U}(k)$ , and  $D \in \mathbb{R}^{k \times k}$  is diagonal. Then,

$$\|C^T X\|_F^2 = \text{tr} \left( X^T C C^T X \right) = \text{tr} \left( X^T U D^2 U^T X \right).$$

The trace quadratic form is maximized at  $X^* = UR$ , for any orthogonal matrix  $R \in \mathcal{U}(k)$ . In particular, when  $R = V$ ,  $X^* = \text{polar}(C)$ .  $\blacksquare$

## B. Sparse CCA

Consider two data matrices that contain  $n$  observations of  $p$  and  $q$  random variables,  $A \in \mathbb{R}^{n \times p}$  and  $B \in \mathbb{R}^{n \times q}$ , whose columns are centered and scaled (i.e., have zero mean and unit standard deviation). We are interested in the ‘‘relationship’’ between the two sets of variables (Hotelling, 1936). CCA finds two linear transformations for the  $p$  variables in  $A$  and the  $q$  variables in  $B$  that maximize the correlations (or equivalently the covariance) between the transformed data,  $\text{Cov}(AZ, BY)$ . Due to the centered and scaled assumption, CCA is equivalent to the following maximization problem:

$$\underset{Z, Y}{\text{maximize}} \quad \|(AZ)^T BY\|_F \quad \text{subject to } Z \in \mathcal{V}(p, k), Y \in \mathcal{V}(q, k). \quad (18)$$

The assumption  $Z \in \mathcal{V}(p, k)$  ensures that the transformed data  $AZ$  have mutually de-correlated columns. So does the assumption  $Y \in \mathcal{V}(q, k)$  for  $BY$ . For high-dimensional data sets (i.e.,  $p$  and  $q$  are large), it is favorable if both  $Z$  and  $Y$  are sparse. For this, We impose sparsity constraints on  $Z$  and  $Y$  and formulate the sparse CCA problem as follows:

$$\begin{aligned} & \underset{Z, Y}{\text{maximize}} \quad \|Z^T A^T B Y\|_F \\ & \text{subject to} \quad Z \in \mathcal{V}(n, k), \|Z\|_1 \leq \gamma_z, Y \in \mathcal{V}(p, k), \|Y\|_1 \leq \gamma_y. \end{aligned} \quad (19)$$

To solve for (19), let  $X = A^T B$  and replace the  $\ell_2$ -equality constraints with their convex hull (i.e.,  $\ell_2$ -inequality constraints). This results in the same formulation for the SMA of  $X$  as in (11). Hence, Algorithm 3 can be applied to solve for sparse CCA.

## C. Cross-validation for Selecting Parameters

We provide a schema for cross-validate the parameters of SCA and SMA (e.g., the approximation rank  $k$  and the sparsity parameter  $\gamma$ ). To assess a candidate parameter, we adapt a  $K$ -fold cross-validation framework ( $K$  often takes the value 10) as previously introduced by Wold (1978):

- (a) Given the input data  $X \in \mathbb{R}^{n \times p}$ , we first construct  $K$  leave-out data matrices  $X^{(1)}, X^{(2)}, \dots, X^{(K)} \in \mathbb{R}^{n \times p}$ , each of which has one- $K$ th disjoint portion of elements being randomly sampled and removed (i.e., set to zero). Let  $C^{(k)}$  collect the indices of those left-out elements in  $X^{(k)}$ , for  $k = 1, 2, \dots, K$ .

- (b) Next, we apply SCA (or the SMA) to every new matrix  $X^{(k)}$  with the candidate tuning parameters and obtain its low-rank approximation  $\hat{X}^{(k)}$ . That is, for SCA,  $\hat{X}^{(k)} = X^{(K)}\hat{Y}^{(k)}[\hat{Y}^{(k)}]^\top$ , and for SMA,  $\hat{X}^{(k)} = \hat{Z}^{(k)}\hat{B}^{(k)}[\hat{Y}^{(k)}]^\top$
- (c) Finally, calculate the mean square error (MSE) of  $\hat{X}^{(k)}$  over those left-out elements  $C^{(k)}$ , defined as

$$\text{MSE}(k) = \sum_{(i,j) \in C^{(k)}} \left( \hat{X}_{ij}^{(k)} - X_{ij} \right)^2, k = 1, 2, \dots, K.$$

We then evaluate the “goodness” of a candidate parameter by the average MSE across  $K$  leave-out data matrices.

Upon the construction of leave-out data matrices, the left-out elements are randomly sampled; this typically removes scattered entries of  $X$ , rather than trunks of adjacent ones. For example, if  $X$  is the adjacency matrix of a graph, then this procedure is akin to the edge cross-validation studied by Li et al. (2020). Setting the left-out elements to zero eliminates all terms in  $\|Z^\top XY\|_F$  that related to them. Our low-rank estimation for the missing entries is closely related to the SVD-based methods in data imputation literature (Troyanskaya et al., 2001).

#### D. Theoretical Guarantees for Soft-thresholding

We provide theoretical guarantees for the soft-thresholding, regarding preservation of orthogonality and the explained variance. Let  $Y \in \mathcal{V}(p, k)$  and let  $\hat{Y} = T_\gamma(Y)$  be the result of soft-thresholding  $Y$  as defined in (15).

First, we denote the included angles between any two columns of  $\hat{Y}$  and  $Y$  as  $\theta_{ij}$ , for  $i, j = 1, 2, \dots, k$ . When it is clear, we also write  $\theta_{ii}$  as  $\theta_i$  for simplicity. We define the *deviation* between  $\hat{Y}$  and  $Y$  as  $\sum_{i=1}^k \sin^2(\theta_i)$ . The following proposition bounds the sum of deviations.

**Proposition 5 (Deviation due to soft-thresholding)** *If  $t$  is sufficiently small, then*

$$\sum_{j=1}^k \sin^2(\theta_j) \leq \|\hat{Y} - Y\|_F^2.$$

**Proof** Let  $\hat{y}_i$  and  $y_i$  be the  $i$ th column of  $\hat{Y}$  and  $Y$  respectively. For the included angle  $\theta_i$ ,

$$\begin{aligned} \cos(\theta_i) &= \hat{y}_i^\top y_i / \|\hat{y}_i\|_2 \\ &= \|\hat{y}_i\|_2 + \hat{y}_i^\top (y_i - \hat{y}_i) / \|\hat{y}_i\|_2 \\ &> \|\hat{y}_i\|_2. \end{aligned}$$

The last inequality results from the definition of soft-thresholding. Then, by the Pythagorean trigonometric identity, we have

$$\begin{aligned} \sin^2(\theta_i) &= 1 - \cos^2(\theta_i) \\ &< 1 - \|\hat{y}_i\|_2^2 \\ &\leq \|\hat{y}_i - y_i\|_2^2. \end{aligned}$$

The last inequality is due to the triangular inequality. Finally, summing over the columns yields the desired result. ■

Proposition 5 controls the deviation with the Frobenius norm of  $Y - \hat{Y}$ . Since the columns of  $Y$  are mutually orthogonal, for any two columns of  $\hat{Y}$ , we have

$$|\hat{y}_i^\top \hat{y}_j| \leq \sin(\theta_j + \theta_i) \|\hat{y}_i\|_2 \|\hat{y}_j\|_2$$

assuming  $\theta_i + \theta_j \leq \pi/2$ . Hence, a small deviation indicates that the orthogonality of  $\hat{Y}$  is conserved after soft-thresholding.

Next, we investigate the change in explained variation due to soft-thresholding. Recall from Section 3.1 that for a data matrix  $X$  and some loadings  $Y$ , the EV is defined as  $\text{EV}(Y) = \|XY\|_F$ . The following proposition bounds the EV for  $\hat{Y}$  and is due to the Theorem 13 in Hu et al. (2016).

**Proposition 6 (Explained variance after soft-thresholding)** *If for all  $1 \leq i \leq k$ ,  $\theta_i = \theta$  and  $\sum_{j=1}^k \cos(\theta_{ij}) \leq 1$ , then*

$$\left(\cos^2 \theta - \sqrt{k-1} \sin 2\theta\right) \text{EV}(Y) \leq \text{EV}(\hat{Y})$$

for any data matrix  $X$ .

Proposition 6 implies that if the deviation between  $Y$  and  $\hat{Y}$  is small, then the EV of  $\hat{Y}$  is close to that of  $Y$ ,

$$\left(\cos^2 \theta - \mathcal{O}(\theta)\right) \text{EV}(Y) \leq \text{EV}(\hat{Y}).$$

## E. Blind Source Separation with SCA

We apply SCA to the blind source separation of image data (Comon and Jutten, 2010). For example, suppose the source signals are individual images, and a sensor senses several mixed images, each an linear mixture of the sources. The objective is then to identify the source images from the observed ones (i.e., to decipher the linear coefficients).

We selected three  $512 \times 512$ -pixels pictures of diverse genres from the internet (Figure 8, the first row). The sample excess kurtosis of the images are 1.53, 3.32, and -0.45 respectively. Next, we generated three ( $n = 3$ ) mixtures of the original images, with the linear coefficients randomly drawn from the uniform distribution,  $\text{Unif}(0,1)$ . The three mixed images are displayed in the second row of Figure 8. For sparse PCA, we vectorize the mixed images (that is  $512^2$ -pixels) and put them in a shallow matrix  $X \in \mathbb{R}^{n \times p}$ , where  $p = 262,144$ . This matrix is then input to SCA (Algorithm 2) for three sparse PCs ( $k = 3$ ), with the sparsity parameter  $\gamma$  set to  $\sqrt{nk}$ . The resulting sparse loadings  $Y \in \mathbb{R}^{p \times k}$  contains the three separated source images and the scores  $S \in \mathbb{R}^{n \times k}$  decodes the mixing coefficients. The third row in Figure 8 displays the three separated images (i.e., the three rows of  $Y$ .) The clean-cut identification of the source images suggests that sparse PCA is capable of extracting sparse and independent components from the data.

## References

- Arash A Amini and Martin J Wainwright. High-dimensional analysis of semidefinite relaxations for sparse principal components. *The Annals of Statistics*, 37(5B):2877–2921, 2009.
- James Baglama and Lothar Reichel. Augmented implicitly restarted lanczos bidiagonalization methods. *SIAM Journal on Scientific Computing*, 27(1):19–42, 2005.



Figure 8: Blind image signal separation using SCA. The three panel rows display three source images, three linear mixtures of the source images, and the three separated images using SCA.

Maayan Baron, Adrian Veres, Samuel L Wolock, Aubrey L Faust, Renaud Gaujoux, Amedeo Vetere, Jennifer Hyoje Ryu, Bridget K Wagner, Shai S Shen-Orr, Allon M Klein, et al. A single-cell transcriptomic map of the human and mouse pancreas reveals inter- and intra-cell population structure. *Cell Systems*, 3(4):346–360, 2016.

Anthony J Bell and Terrence J Sejnowski. The “independent components” of natural scenes are edge filters. *Vision Research*, 37(23):3327–3338, 1997.

Coen A Bernaards and Robert I Jennrich. Gradient projection algorithms and software for arbitrary rotation criteria in factor analysis. *Educational and Psychological Measurement*, 65(5):676–696, 2005.

Quentin Berthet and Philippe Rigollet. Optimal detection of sparse principal components in high dimension. *The Annals of Statistics*, 41(4):1780–1815, 2013.

T Tony Cai, Zongming Ma, and Yihong Wu. Sparse PCA: Optimal rates and adaptive estimation. *The Annals of Statistics*, 41(6):3074–3110, 2013.

John B Carroll. An analytical solution for approximating simple structure in factor analysis. *Psychometrika*, 18(1):23–38, 1953.

Aiyou Chen and Peter J Bickel. Efficient independent component analysis. *The Annals of Statistics*, 34(6):2825–2855, 2006.

- Fan Chen, Yini Zhang, and Karl Rohe. Targeted sampling from massive block model graphs with personalized pagerank. *Journal of the Royal Statistical Society: Series B (Statistical Methodology)*, 82(1):99–126, 2020.
- Pierre Comon. Independent component analysis, a new concept? *Signal Processing*, 36(3):287–314, 1994.
- Pierre Comon and Christian Jutten. *Handbook of Blind Source Separation: Independent component analysis and applications*. Academic Press, Oxford, UK, 2010.
- Alexandre d’Aspremont, Laurent El Ghaoui, Michael I Jordan, and Gert R G Lanckriet. A direct formulation for sparse PCA using semidefinite programming. *SIAM Review*, 49(3):434–448, 2007.
- David L Donoho. De-noising by soft-thresholding. *IEEE Transactions on Information Theory*, 41(3):613–627, 1995.
- David J Field. Relations between the statistics of natural images and the response properties of cortical cells. *Journal of the Optical Society of America A*, 4(12):2379–2394, 1987.
- David J Field. What is the goal of sensory coding? *Neural Computation*, 6(4):559–601, 1994.
- Santo Fortunato. Community detection in graphs. *Physics Reports*, 486(3-5):75–174, 2010.
- Milana Gataric, Tengyao Wang, and Richard J. Samworth. Sparse principal component analysis via axis-aligned random projections. *Journal of the Royal Statistical Society: Series B (Statistical Methodology)*, 82(2):329–359, 2020. doi: 10.1111/rssb.12360. URL <https://rss.onlinelibrary.wiley.com/doi/abs/10.1111/rssb.12360>.
- Karol Gregor and Yann LeCun. Learning fast approximations of sparse coding. In *Proceedings of the 27th International Conference on International Conference on Machine Learning, ICML’10*, page 399–406, Madison, WI, USA, 2010. Omnipress.
- Paul W Holland, Kathryn Blackmond Laskey, and Samuel Leinhardt. Stochastic blockmodels: First steps. *Social Networks*, 5(2):109–137, 1983.
- Roger A Horn and Charles R Johnson. *Matrix Analysis*. Cambridge University Press, Cambridge, UK, 1985.
- Harold Hotelling. Analysis of a complex of statistical variables into principal components. *Journal of Educational Psychology*, 24(6):417, 1933.
- Harold Hotelling. Relations between two sets of variates. *Biometrika*, 28(3-4):321–377, 1936.
- Zhenfang Hu, Gang Pan, Yueming Wang, and Zhaohui Wu. Sparse principal component analysis via rotation and truncation. *IEEE Transactions on Neural Networks and Learning Systems*, 27(4):875–890, 2016.
- Aapo Hyvarinen. Fast and robust fixed-point algorithms for independent component analysis. *IEEE Transactions on Neural Networks*, 10(3):626–634, 1999.

- Aapo Hyvärinen and Erkki Oja. Independent component analysis: algorithms and applications. *Neural Networks*, 13(4-5):411–430, 2000.
- JNR Jeffers. Two case studies in the application of principal component analysis. *Journal of the Royal Statistical Society: Series C (Applied Statistics)*, 16(3):225–236, 1967.
- Robert I Jennrich. A simple general procedure for orthogonal rotation. *Psychometrika*, 66(2): 289–306, 2001.
- Iain M Johnstone and Arthur Yu Lu. On consistency and sparsity for principal components analysis in high dimensions. *Journal of the American Statistical Association*, 104(486):682–693, 2009.
- Ian T Jolliffe. Rotation of principal components: choice of normalization constraints. *Journal of Applied Statistics*, 22(1):29–35, 1995.
- Ian T Jolliffe, Nickolay T Trendafilov, and Mudassir Uddin. A modified principal component technique based on the LASSO. *Journal of Computational and Graphical Statistics*, 12(3): 531–547, 2003.
- Michel Journée, Yurii Nesterov, Peter Richtárik, and Rodolphe Sepulchre. Generalized power method for sparse principal component analysis. *Journal of Machine Learning Research*, 11: 517–553, 2010.
- Henry F Kaiser. The varimax criterion for analytic rotation in factor analysis. *Psychometrika*, 23 (3):187–200, 1958.
- Henry F Kaiser. The application of electronic computers to factor analysis. *Educational and Psychological Measurement*, 20(1):141–151, 1960.
- Honglak Lee, Alexis Battle, Rajat Raina, and Andrew Y Ng. Efficient sparse coding algorithms. In *Proceedings of the 19th International Conference on Neural Information Processing Systems, NIPS’06*, page 801–808, Cambridge, MA, USA, 2006. MIT Press.
- Tianxi Li, Elizaveta Levina, and Ji Zhu. Network cross-validation by edge sampling. *Biometrika*, 04 2020. ISSN 0006-3444. doi: 10.1093/biomet/asaa006.
- Lester Mackey. Deflation methods for sparse PCA. In *Proceedings of the 21st International Conference on Neural Information Processing Systems, NIPS’08*, page 1017–1024, Red Hook, NY, USA, 2008. Curran Associates Inc.
- Kanti V Mardia. Measures of multivariate skewness and kurtosis with applications. *Biometrika*, 57 (3):519–530, 1970.
- Jari Miettinen, Sara Taskinen, Klaus Nordhausen, and Hannu Oja. Fourth moments and independent component analysis. *Statistical Science*, 30(3):372–390, 2015.
- Baback Moghaddam, Yair Weiss, and Shai Avidan. Generalized spectral bounds for sparse LDA. In *Proceedings of the 23rd International Conference on Machine Learning, ICML ’06*, page 641–648, New York, NY, USA, 2006. Association for Computing Machinery.

- Daniel T Montoro, Adam L Haber, Moshe Biton, Vladimir Vinarsky, Brian Lin, Susan E Birket, Feng Yuan, Sijia Chen, Hui Min Leung, Jorge Villoria, et al. A revised airway epithelial hierarchy includes CFTR-expressing ionocytes. *Nature*, 560(7718):319–324, 2018.
- Jorge Nocedal and Stephen Wright. *Numerical Optimization*. Springer Science & Business Media, New York, NY, USA, second edition, 2006.
- Bruno A Olshausen and David J Field. Emergence of simple-cell receptive field properties by learning a sparse code for natural images. *Nature*, 381(6583):607, 1996.
- Karl Pearson. On lines and planes of closest fit to systems of points in space. *The London, Edinburgh, and Dublin Philosophical Magazine and Journal of Science*, 2(11):559–572, 1901.
- Lindsey W Plasschaert, Rapolas Žilionis, Rayman Choo-Wing, Virginia Savova, Judith Knehr, Guglielmo Roma, Allon M Klein, and Aron B Jaffe. A single-cell atlas of the airway epithelium reveals the CFTR-rich pulmonary ionocyte. *Nature*, 560(7718):377–381, 2018.
- Tai Qin and Karl Rohe. Regularized spectral clustering under the Degree-Corrected Stochastic Blockmodel. In *Proceedings of the 26th International Conference on Neural Information Processing Systems*, NIPS’13, page 3120–3128, Red Hook, NY, USA, 2013. Curran Associates Inc.
- Karl Rohe and Muzhe Zeng. Vintage factor analysis with varimax performs statistical inference, 2020. arXiv:2004.05387 [stat.ME].
- Karl Rohe, Tai Qin, and Bin Yu. Co-clustering directed graphs to discover asymmetries and directional communities. *Proceedings of the National Academy of Sciences*, 113(45):12679–12684, 2016.
- Richard J Samworth and Ming Yuan. Independent component analysis via nonparametric maximum likelihood estimation. *The Annals of Statistics*, 40(6):2973–3002, 2012.
- Dan Shen, Haipeng Shen, and James Stephen Marron. Consistency of sparse PCA in high dimension, low sample size contexts. *Journal of Multivariate Analysis*, 115:317–333, 2013.
- Haipeng Shen and Jianhua Z Huang. Sparse principal component analysis via regularized low rank matrix approximation. *Journal of Multivariate Analysis*, 99(6):1015–1034, 2008.
- Louis Leon Thurstone. Multiple factor analysis. *Psychological Review*, 38(5):406, 1931.
- Robert Tibshirani. Regression shrinkage and selection via the lasso. *Journal of the Royal Statistical Society. Series B (Methodological)*, pages 267–288, 1996.
- Andreas M Tillmann and Marc E Pfetsch. The computational complexity of the restricted isometry property, the nullspace property, and related concepts in compressed sensing. *IEEE Transactions on Information Theory*, 60(2):1248–1259, 2014.
- Olga Troyanskaya, Michael Cantor, Gavin Sherlock, Pat Brown, Trevor Hastie, Robert Tibshirani, David Botstein, and Russ B Altman. Missing value estimation methods for DNA microarrays. *Bioinformatics*, 17(6):520–525, 2001.



- Vincent Q Vu and Jing Lei. Minimax sparse principal subspace estimation in high dimensions. *The Annals of Statistics*, 41(6):2905–2947, 2013.
- Vincent Q Vu, Juhee Cho, Jing Lei, and Karl Rohe. Fantope projection and selection: A near-optimal convex relaxation of sparse PCA. In *Proceedings of the 26th International Conference on Neural Information Processing Systems, NIPS’13*, page 2670–2678, Red Hook, NY, USA, 2013. Curran Associates Inc.
- Tengyao Wang, Quentin Berthet, and Richard J Samworth. Statistical and computational trade-offs in estimation of sparse principal components. *The Annals of Statistics*, 44(5):1896–1930, 2016.
- Daniela M Witten, Robert Tibshirani, and Trevor Hastie. A penalized matrix decomposition, with applications to sparse principal components and canonical correlation analysis. *Biostatistics*, 10(3):515–534, 2009.
- Svante Wold. Cross-validatory estimation of the number of components in factor and principal components models. *Technometrics*, 20(4):397–405, 1978.
- Xiao-Tong Yuan and Tong Zhang. Truncated power method for sparse eigenvalue problems. *Journal of Machine Learning Research*, 14(1):899–925, 2013.
- Yilin Zhang and Karl Rohe. Understanding regularized spectral clustering via graph conductance. In *Advances in Neural Information Processing Systems*, pages 10631–10640, 2018.
- Yini Zhang, Fan Chen, and Karl Rohe. Networked public opinion as flocks in a murmuration. In preparation, 2020.
- Hui Zou and Trevor Hastie. Regularization and variable selection via the elastic net. *Journal of the Royal Statistical Society: Series B (Statistical Methodology)*, 67(2):301–320, 2005.
- Hui Zou and Lingzhou Xue. A selective overview of sparse principal component analysis. *Proceedings of the IEEE*, 106(8):1311–1320, 2018.
- Hui Zou, Trevor Hastie, and Robert Tibshirani. Sparse principal component analysis. *Journal of Computational and Graphical Statistics*, 15(2):265–286, 2006.